CHAPTER 3

THE LR REPRESENTATION OF PARTICLES

The Analysis of the Stern-Gerlach Experiment

QuWT-c3-220417

Reference [102]-C presented the fundamentals of a particular locally real representation of quantum mechanics, LR. In the present work, we extend LR to a more inclusive representation that treats the "non-observables" of empty waves that are generated during condensation processes of photons and particles. See section 1.1. The following sections focus on a more inclusive LR representation of particles with particular emphasis in the context of the 1922 Stern-Gerlach experiment, SGE. [390]

The locally real 3-dimensional wave packet structures of photons and particles are shown in [102]-C to be substantially different. Correspondingly, macroscopic devices such as calcite polarizers and Stern-Gerlach magnets for measuring the respective quantum states of photons and particles are also substantially different.

Despite those differences, there are profound mathematical homologies in the condensation processes that occur during the respective measurement processes and in the ensemble-distribution of output states. These homologies contribute to the perception by the Probabilistic Interpretation of quantum mechanics, PI, that the standard form of the wave function is sufficient in the complete representation of physical phenomena, albeit in a probabilistic (non-real) and non-local manner.

In the foregoing sections we examined those condensation processes and ensemble-distributions in detail for photons. In the present section we examine the particular aspects of particle measurement imposed by LR that result in those homologies with photons.

In PI the wave packet of a particle such as the spin 1/2 electron in free space is represented by an oscillatory amplitude and an intensity envelope represented one-dimensionally in Fig. 3.1. In LR the electron is more completely represented by a coherence wave of objectively real spin
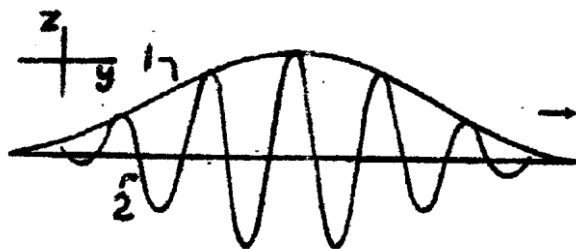
Fig. 3.1. A simplistic one-dimensional representation of a particle wave packet in the probabilistic interpretation, PI.

structures. The mass-bearing, particle-like electron and its associated magnetic moment $\mathbf{\mu}_e$ reside on one constituent spinor of one of the spin structures as depicted in the Fig. 3.2a representation of the wave packet that shows only a sampling of the constituent spin structures. For purposes of visual clarity Fig. 3.2a is a one-dimensional representation of a sampling of constituent spin structures and only the single electron-occupied spinor is depicted.

A bisecting cross section of a single spin structure of the electron's coherence wave packet is depicted in Fig. 3.3. That depicted cross section happens to be of the "occupied" spin structure, i.e. the particular spin structure that includes the single spinor occupied by the particle-like electron. That bisecting cross section is inclusive of the pole orientation θ_p, ϕ_p of the spin structure hemisphere in a spherical coordinate frame and, solely for instructional purposes, atypically also includes the mass-bearing "occupied" spinor at θ_M, ϕ_M since in general $\phi_p \neq \phi_M$. (The orientations of "observables" such as the particle mass M are denoted by capitalized subscripts while the orientations of the "non-observables" such as the pole of the spin structure, p, are identified by lower case subscripts. Applying that convention to photon wave packets, the arc bisector orientation is θ_a and the instantaneous energy quantum orientation on that arc is θ_E.)
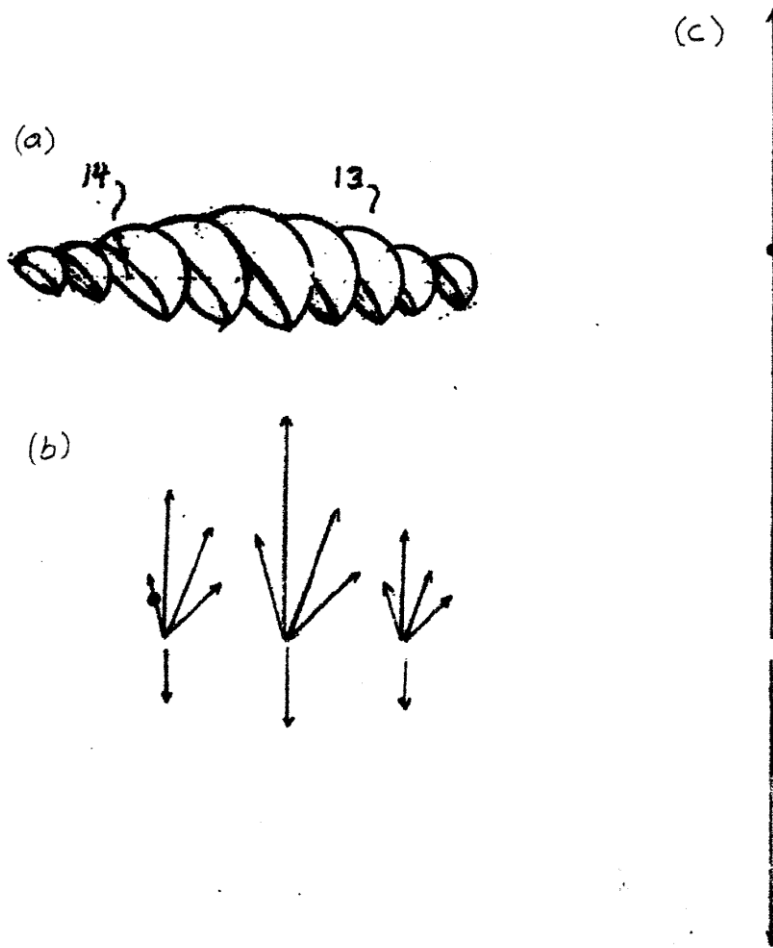
Fig. 3.2a-c. (a) is a simplistic one-dimensional representation of an LR particle wave packet comprised of a coherence wave of spin structures and is an analog to the PI particle wave packet in Fig. 3.1. Under a condensation process the spatial extent of (a) diminishes and concurrently the constituent spin structures projectively condense to orthogonal spinors as depicted intermediately in (b) and to completion in (c).
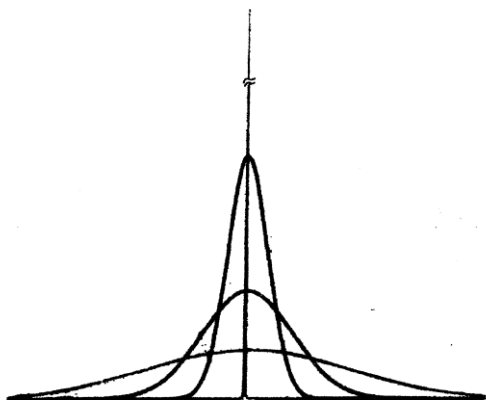
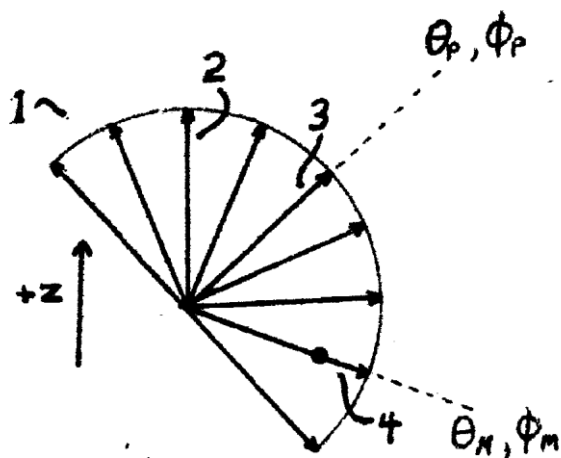*Fig. 3.2d. Spatial probability distributions during condensation.*

Fig. 3.3. A bisecting cross section of a single spin structure that untypically includes the pole orientation spinor and mass-bearing spinor.

We shall show below that when the electron wave packet suddenly encounters a substantial magnetic field the entire wave packet of spin structures and the spin structures themselves abruptly concurrently condense to a Dirac delta-like single spinor occupied by the particle-like electron that is aligned with the magnetic field. For a free electron that concurrent condensation is depicted in the sequence Fig's. 3.2a→b. The accompanying Fig. 3.2d is a representation of the spatial probability

distributions during the condensation. In that process, the spatially unbounded wave packet of spin structures for a free electron shown in Fig. 3.2a is initially Gaussian and remains Gaussian as the its characteristic length diminishes during the suddenly induced condensation. Although an LR analysis here of free particle interactions with magnetic field with respect to spin quantization would most directly analogously complement our LR analysis of (free) photon interaction with polarizers, it is far more instructive to instead analyze those particle interactions with respect to atomically bound electrons as used in the original SGE. Parenthetically, applying the analysis to atomically bound electrons as opposed to free electrons avoids the complication of treating ancillary Lorentz forces but that choice does not exclude generalization of the analysis to free particles.

3.1 DIRECTIONAL QUANTIZATION AND LONGITUDINAL GRADIENT FIELDS

Before proceeding to a detailed examination of atomically bound states as they progress through the gradient fields of the SGE magnet we first examine the requisite gradient fields for producing the experimentally observed "directional quantization" of those bound states from the perspective of LR. In the SGE, a beam of randomly oriented silver (Ag) atoms is directed toward a gradient magnet shown in Fig. 3.4a and directional quantization of the bound states is associated with the splitting of the atomic beam as it traverses the magnetic field. The magnet's "lower" pole face includes an apex ridge along that produces a strong gradient field proximal to the apex. The "upper" pole is flat except for a 3 mm wide and 30 mm deep rectangular groove opposing the apex ridge on the lower pole face. The lower pole's 70° apex and the upper pole's flat region are separated by 2 mm. The atomic Ag beam is directed at ~1000 m/s along a trajectory <1 mm above that apex where it experiences a transverse field strength of ~10^4 Gauss as well as a strong transverse gradient field ~10^3 Gauss/mm. [383-384] Fig. 3.4b is a cross section of the Fig. 3.4a perspective view of the SGE magnet in which particular segments along the beam path are identified. Fig. 3.4c is an approximate representation of the corresponding magnetic field B(y) along the Fig. 3.4b beam path showing the field inflections within beam segments 11, 13, 15 and 17 characteristic of an opposed pole magnet.

QuWT

The energetics mechanism of the randomly oriented incident μ_e transitioning to alignment with +B (along +z) or –B (along –z) is not directly addressed by PI. Rather, that transition is presented as an ad hoc outcome associated with the measurement of μ_e relative to the B axis, a measurement which is inherently required by PI to yield discrete quantized values. Nevertheless, this lack of a transition mechanism in SGE is commonly identified as a quintessential example of the "measurement problem" endemic to PI. [382] [384]

Shortly after the directional quantization results of SGE were reported in 1922, Ehrenfest hypothesized in communications with Einstein that the energetics mechanism was associated with a sudden "schock" (shock) as the electron entered the field of the magnet. This particular speculation was not pursued in a paper that Ehrenfest and Einstein published shortly thereafter that sought without success to identify a viable energetics mechanism for directional quantization. [383] Heisenberg proposed several years later in 1927 that the rotation of the electron's magnetic moment μ_e to alignment with the magnetic field is caused by a "schütteln" (jolting) mechanism, most likely a sudden process analogous to Ehrenfest's shock hypothesis. In either case a viable mechanism for the sudden process would necessitate the identification of an operant force acting over some finite time. A satisfactory formulation of that mechanism has continued to be elusive for a century. [382] [384]

 A sudden process is the essential starting point for an LR-based energetics mechanism that produces the directional quantization observed in SGE. In our LR analysis of the SGE with regard to the underlying basis of directional quantization we also examine the 1929 Rabi experiment [385] since the latter also demonstrates directional quantization but does so solely from a longitudinal gradient that is largely exterior to the magnet's pole perimeter.

Directional quantization for the SGE magnet is commonly associated with its characteristic transverse gradient magnetic field within its pole perimeter. In the following we show that the SGE magnet also has an exterior longitudinal gradient comparable to that of the Rabi magnet and propose that the underlying basis of directional quantization for the SGE is fundamentally related to its longitudinal gradient whereas its transverse gradient is secondary to that basis.
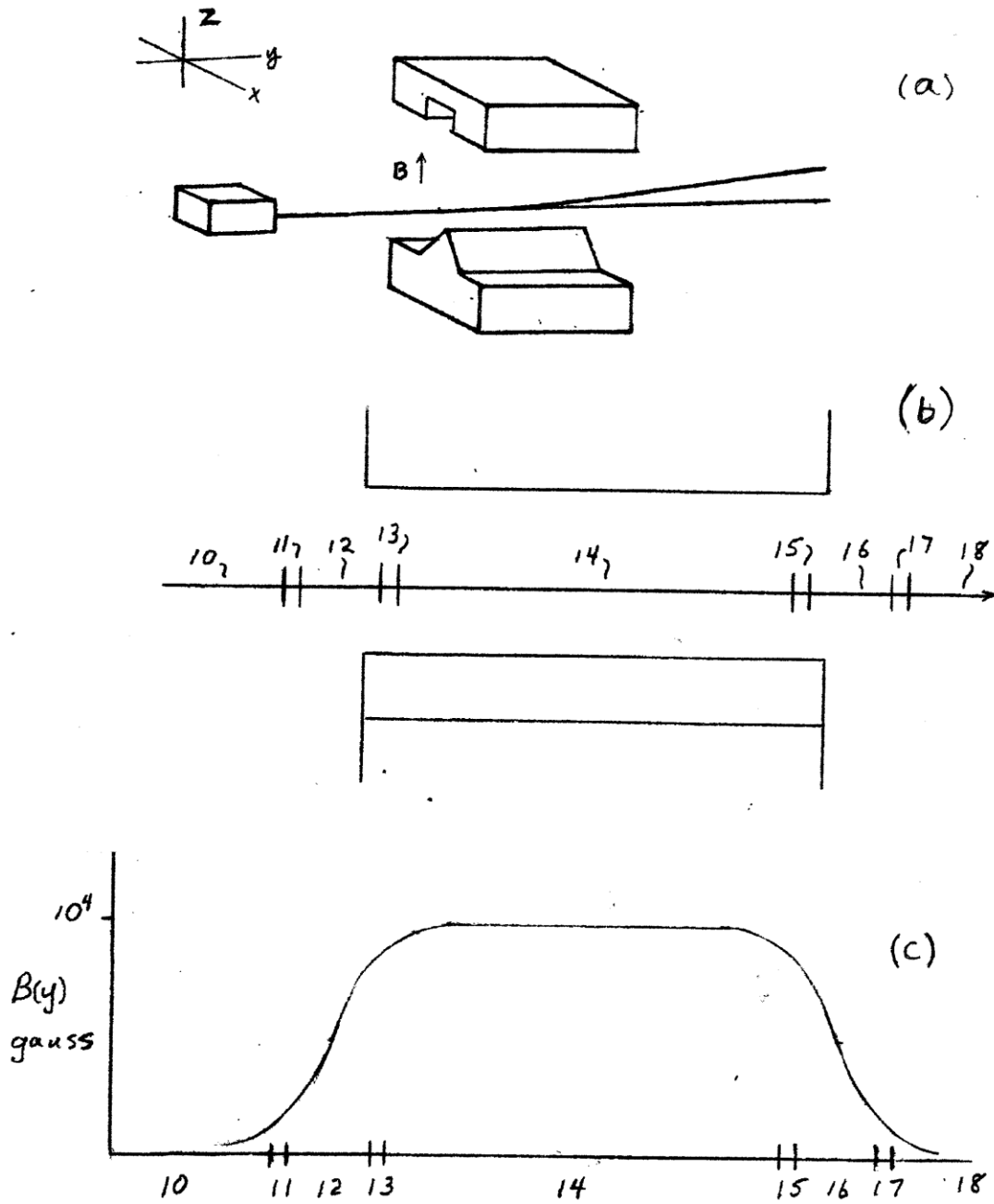
Fig. 3.4a-c. (a) shows a perspective view of a SGE beam source and magnet. Only upwardly deflected atoms in the beam are depicted. Empty electron waves are undeflected. (b) is a side view of the SGE magnet and significant segments along the beam path. (c) is the magnetic field along the beam path relative to those segments.

Because of the relevance of the Rabi experiment to the SGE we briefly detour to an analysis of Rabi's experiment from the perspective of LR. The Rabi experiment magnet simply consists of opposed flat rectangular poles separated by 2 mm with an Ag beam directed through the pole gap on the plane bisecting that gap. Fig. 3.5a is a top view of the magnet and beam path with the "upper" pole removed. The field is a uniform 10^4 Gauss for all regions on that plane within the magnet that are 2 mm or more distal from the pole edges. For purposes of achieving directional quantization the Rabi experiment makes explicit use of the high gradient naturally provided by the fringe field that extends from ~4 mm outside the pole perimeter to ~2 mm inside the pole perimeter. Because of symmetry considerations, the fringe field **B** vectors are normal to the bisector plane and the fringe field constitutes a longitudinal high gradient with respect to a beam directed on that plane toward the magnet.

The fields of the Rabi magnet along the y axis on that bisector plane and of the SGE magnet on its beam path are very similar despite the differences in the respective magnet designs. Fig. 3.5b depicts B(y) in the bisector plane for the Rabi magnet. The pole gap of Rabi magnet is 2 mm. For the SGE magnet the gap between the ridge apex of the "lower" pole and the flat region of the opposing "upper" pole is also 2 mm. The uniform field on that bisector plane within the Rabi magnet is ~10^4 Gauss. Along the beam path within the SGE magnet the field is also a relatively constant ~10^4 Gauss (irrespective of a strong gradient normal to that beam path). Both magnets are configured with opposed poles that similarly constrain the respective longitudinal gradient fringe fields that are exterior to the pole perimeters and provide convergence to uniform fields on the beam paths within the pole perimeters. Effectively, the two magnets have fields with similar inflection points that define their respective longitudinal high gradient boundaries and have similar longitudinal gradient fields B(y) along the respective Ag beam paths.
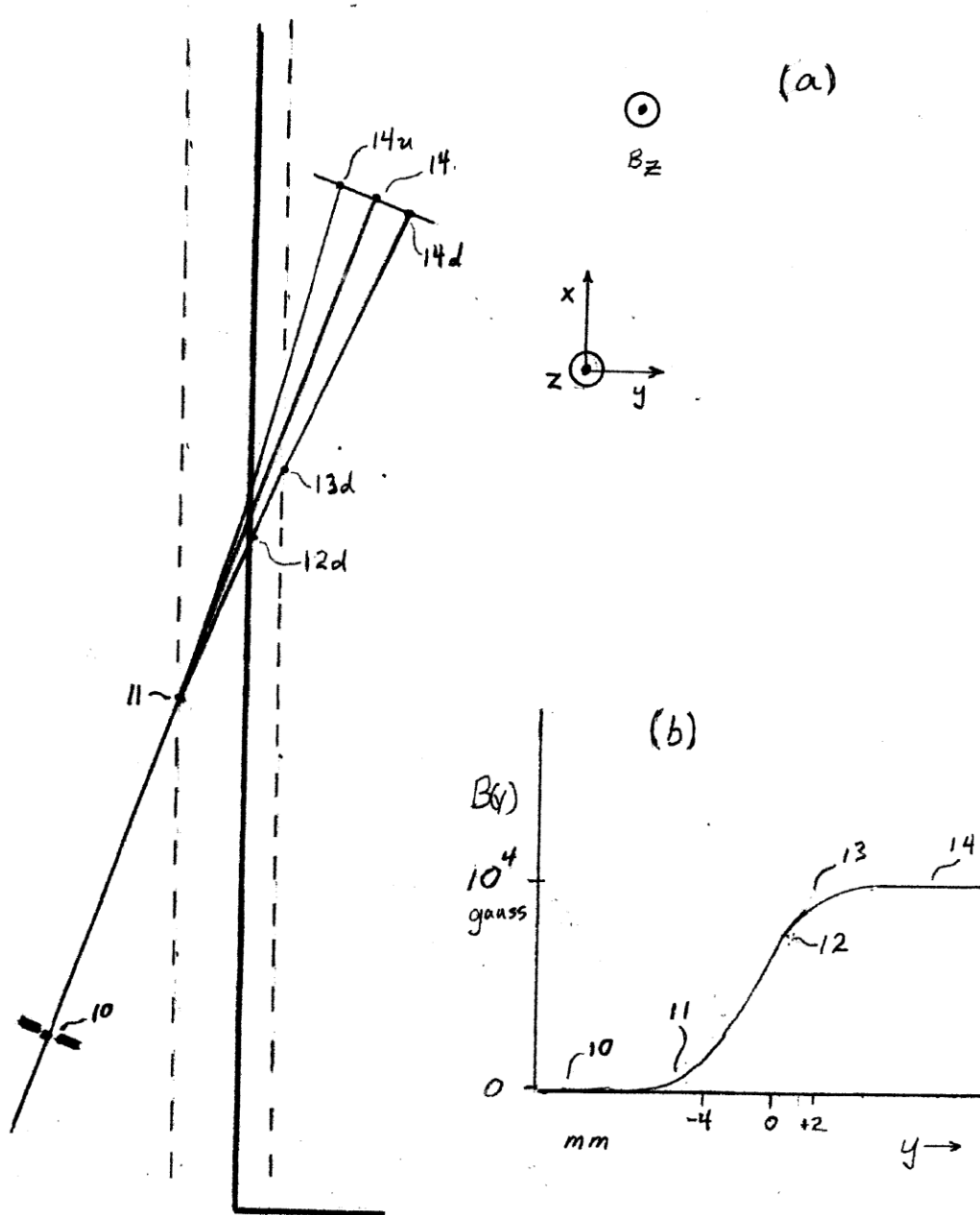
QuWT

Fig. 3.5a-b. (a) shows the Rabi experiment and the beam path. (b) shows the magnetic field along the y axis in the plane located between the magnet poles.

QuWT

The velocity of the Ag beam in the Rabi experiment is the same as that for the SGE, ~1000 m/s. However, because the Ag beam is directed on the Rabi magnet pole bisector plane at 80° from the normal to the pole edges, the velocity component through the gradient field is only 1000 cos 80° m/s=170 m/s. Then the 1000 m/s velocity of electron wave packets through the SGE longitudinal gradient field far exceeds the 170 m/s velocity component along the y axis through the comparable Rabi magnet longitudinal gradient field.

Importantly, the geometry and methodology of the Rabi experiment provides for a highly accurate absolute quantitative confirmation of μ_e, to about 1 part in 500, from measurement of the beam split and from an accurate measurement of the average field traversed by the beam based upon field measurements at the beginning and at the end of the beam path. For the SGE accuracy for the measurement of μ_e is more problematic because of the indeterminacy of the B field experienced by the Ag beam within the transverse gradient.

From the perspective of LR, the Rabi experiment shows that the sudden process of directional quantization occurs at or before the Ag beam entry into the 6 mm longitudinal high gradient field along y since virtually all of the deflective force that occurs on the beam path is confined to that 6 mm high gradient zone. If directional quantization occurs at some point intermediate to pt.10 and pt.11 instead of at pt.11 the observed deflection of the Ag atom at pt. 14d from which μ_e is computed would be the same. Conversely, if the beam path does not fully traverse the 6 mm high gradient field, the resultant beam deflection is diminished and the calculated μ_e is lower than that of independently determined values of μ_e.

(An LR retrospective analysis of the Rabi experiment will show that the deflection either to pt.14u left or to pt.14d right deterministically corresponds respectively to the objectively real polar orientation $\theta_p<90°$ or $>90°$ of the incident electron's spin structures. The u and d notations respectively denote conventional measurements of "spin up" and "spin down" quantum states.)

Because we cannot exclude the possibility that directional quantization may have occurred at some point between pt.10 and pt. 11 at a distance along y greater than 4 mm from the pole perimeter, we conclude that for the Rabi experiment the field characteristics in the neighborhood of the 4 mm exterior

QuWT

boundary provide a sufficiency criterion for inducing directional quantization in electrons denoted as $Q_{e\text{-}s}$ as opposed to the necessary or actual criterion for electrons, denoted simply as Q_e.

That sufficiency criterion $Q_{e\text{-}s}$ is of interest because it can be quantified for the Rabi experiment and can then be applied to the SGE because of the similarities of longitudinal gradient fields for the two experiments. The simple geometry of the Rabi magnet is amenable to analytic representation. For the field exterior to the magnet in the gap bisector plane that representation reduces to the simple expression

$B(y)=h$ arctan (g/y)

where the pole gap dimension $g=2$ mm, h is a scale factor of the magnetic field strength, and $y=0$ mm at the pole edge. At $y=-4$ mm, $B(-4)=1466$ Gauss and $\partial_y B(-4)=370$ Gauss/mm. The scale factor h is found by a commonly applied calculation of the interior $B(y)$ on the bisector plane between opposed flat poles and matching the $B(0)$ perimeter value to that of the exterior $B(0)$ perimeter value.

The relevant suddenness criterion Q for inducing directional quantization is based upon achieving a critical time rate of change of the magnetic field $\partial_t B$ for a particular particle type. For a particle, such as an electron, moving at some velocity $v=\partial y/\partial t$ relative to a static gradient field $\partial B/\partial y$, that criterion is simply some particular value of the product of those quantities at some value of y_{DQ} where directional quantization is estimated to have occurred,

$Q_e=(\partial B(y_{DQ})/\partial y)(\partial y/\partial t)=\partial B(y_{DQ})/\partial t$.

For the Rabi experiment, where the velocity component along y through the fringe gradient is 170 m/s, the criterion

$Q_{e\text{-}s}= \partial_y B(-0.4 \text{ cm}) \, \partial_t y$

   $=3.7 \times 10^3$ gauss/cm$\cdot 1.7 \times 10^4$ cm/s

   $= 6.2 \times 10^7$ gauss/s $\geq Q_e$.

Computed for the pt.11 field inflection at $y=-4$ mm that defines the exterior high gradient boundary, 4 mm distant from the pole perimeter. Clearly, the actual necessary criterion Q_e may be realized at a greater distance along y from that boundary where the gradient is lower.

QuWT

Fig. 3.5b shows the general contour of B(y) where the pole perimeter is located at y=0. Importantly there is a further increase of the gradient beyond the gradient local to the pt.11 inflection. That further increase continues until the pt.13 inflection is approached. Consequently Q_{e-s} is continuously exceeded (along with Q_e) as the electron traverses the increased gradient region between pts.11 and 13. As the neighborhood of the pt.13 inflection at y=+2 mm is traversed a progressively diminishing gradient is encountered that results in a progressively diminishing $\partial_t B$ passing below Q_{e-s}= 6.2×10^7 gauss/s and below Q_e. For still larger y beyond pt.13 the diminishing gradient converges B(y) toward a constant value of 10^4 gauss inside the Rabi experiment magnet at pt.14.

Compared to the Rabi magnet, the SGE magnet does not lend itself to a simple analytical representation of its exterior fringe field. However, as noted above, the similar properties of a 2 mm pole gap and a maximum field of ~10^4 gauss suggest that B(y) and $\partial_y B(y)$ along the respective beam paths are functionally approximately comparable. However, the SGE 10^3 m/s beam velocity through the longitudinal gradient of the SGE magnet is 5.88 times larger than that of the Rabi experiment. As a result, that Q_{e-s}=6.2×10^7 gauss/s sufficiency criterion is achieved at a substantially greater distance from the SGE magnet pole perimeter.

To the approximation that the Rabi and SGE magnets have functionally comparable B(y) along their respective entry beam paths we can then readily solve for the SGE y value that yields the sufficiency criterion. We find that y≈−10 mm, where B(−10)=617 gauss, $\partial_y B(−10)$=−63 gauss/mm and the SGE v=10^3 m/s, substantially gives the Q_{e-s}=6.2×10^7 gauss/s sufficiency criterion for directional quantization.

The principal objective of this exercise in comparing the SGE and the Rabi experiment is to demonstrate that the process of directional quantization for the SGE occurs in the longitudinal gradient exterior to the magnet and not in the transverse gradient that is characteristically associated with the SGE. The transverse gradient is then understood to have the reduced, ancillary role of spatially distinguishing the electrons, which have already been directionally quantized, by providing an upward or a downward deflection.

In this generalization of the Rabi experiment to the SGE with similar longitudinal fields, the expression for the criterion

QuWT

$Q_e = \partial_y B(y_{DQ}) \cdot \partial_t y = \partial_t B(y_{DQ}) = 6.2 \times 10^7$ gauss/s

is presumed to remain valid for the latter since the respective velocities through the longitudinal gradient, $v_y = 1.7 \times 10^4$ cm/s and $v_y = 10^5$ cm/s, differ by less than an order of magnitude.

However, by any measure both of these velocities of electrons, coupled to Ag atoms, are orders of magnitude smaller than that of free electron beams in typical practical applications. Accordingly, the range of validity for the Q_e expression should not be indiscriminately extrapolated to extreme deviations of electron velocity beyond the $v_y = 1.7 \times 10^4$ cm/s in the Rabi experiment.

An example of an underlying basis limiting the validity range of Q_e relates to the duration of the condensation process. That process involves a physically extended coherence wave condensing to point-like δ-forms and is expected to occur over some very small but finite time Δt_c independent of the sudden exterior field perturbation that triggered it. For the extraordinarily slow electron progression through the Rabi and SGE longitudinal gradient, the finite Δt_c can be approximated as an instantaneous event occurring to completion while the electron has progressed no further than the beginning of the longitudinal gradient region. The time for the electron to traverse that entire longitudinal gradient region is then some $\Delta t_g \gg \Delta t_c$.

If the electron velocity is greatly increased to the extent that $\Delta t_g < \Delta t_c$, the condensation process of directional quantization is disrupted. Directional quantization for such large electron velocities can still be accommodated by extending the gradient field length such that minimally $\Delta t_g > \Delta t_c$ to simultaneously ensure that directional quantization is completed within Δt_g and that the resultant anti-aligned δ-forms are at least microscopically separated by the gradient in the remaining Δt_g.

3.2 OUTLINE OF SGE ANALYSIS

We return to an analysis of the SGE with the benefit of some measure of a Q_e criterion for directional quantization. In this analysis we will make extensive use of the enumerated segments along the beam path shown in Fig. 3.4b and the Fig. 3.4c representation of the associated magnetic field along that path. These figures show that the field inflections occur in the short

segments 11, 13, 15, and 17 which we identify as transitional segments. In the longer intervening segments 10, 12, 14, 16, and 18 the wave states are substantially invariant. The processes occurring in these segments are briefly described in the several paragraphs below followed by a more detailed analysis.

● The field-free wave state of an Ag 5s electron on segment 10 is a uniform amplitude coherence wave of spin structures on the 5s orbital.

● As that uniform amplitude coherence wave enters transitional segment 11 it has an encounter with a suddenly changing magnetic field $\partial_t B$ that exceeds Q_e causing the entire wave to rapidly condense to a single Dirac-delta "δ-form" occupied spinor aligned with the SGE magnetic field B as it reaches the end of segment 11. That B-alignment constitutes directional quantization.

● As the electron wave on the 5s orbital enters segment 12 it remains in δ-form and B-alignment throughout the entire longitudinal high gradient field of segment 12 because Q_e is continuously exceeded over that segment. Effectively, the δ-form condensation state is continuously induced over the entire segment where Q_e is exceeded.

● The δ-form electron wave enters transitional segment 13 and reaches a point at which the diminishing gradient causes the electron to experience a $\partial_t B$ below Q_e. At that point the δ-form electron wave is rapidly restored to a state similar to that of the field-free uniform coherence wave of spin structures on the 5s orbital similar on segment 10. However, because of the continued presence of the substantial B field during that restoration transition the particle-like electron on the restored uniform coherence wave of spin structures remains in B-alignment as it exits segment 13.

● The restored uniform coherence wave of the 5s electron is unaltered as it enters and traverses segment 14. The only consequential outcome is a small but measurable 0.1 mm deflection from the initial beam path because of the high $\partial_z B \approx 10^4$ gauss/mm transverse gradient acting upon the B-aligned electron.

● The restored uniform coherence wave with a B-aligned electron exits segment 14 and enters segment 15 where it passes a point at which the magnitude of the negative $\partial_t B$ exceeds Q_e. From the perspective of symmetry considerations, the sudden process of condensation that occurs

QuWT

as a coherence wave of spin structures in a low field enters some $\partial_y B$, as in segment 11, is also expected to occur for that coherence wave in a high field as it enters the negative of that same $\partial_y B$ as in segment 15. In both cases it is the magnitude of a sudden ΔB change that induces condensation and not the sign of that change. More generally, the criterion Q_e is relates to a magnitude $|\partial_t B|$ and is not dependent on the sign of the $\partial_t B$. Consequently, condensation occurs in segment 15 producing a transition to a δ-form occupied spinor in B-alignment on that segment.

● The occupied δ-form spinor exits segment 15 and enters the (negative) high gradient on segment 16 where Q_e is continuously exceeded. As a result the δ-form occupied spinor is substantially unaltered as it traverses segment 16 and enters segment 17.

● In segment 17 the occupied δ-form spinor reaches a point at which the magnitude of the diminishing gradient causes the $\partial_t B$ value to fall below Q_e and the occupied δ-form spinor is rapidly restored to a state similar to that of the uniform coherence wave of spin structures on segment 14. Notably however, because B~0 after that restoration transition, the particle-like electron on the restored uniform coherence wave of spin structures is not energetically constrained to remain in B-alignment (as it was upon exiting segment 13).

● The restored uniform coherence wave that exits segment 17 and traverses segment 18 is very similar to the initial wave on segment 10. Both have the same polarization condition of either $\theta_p < 90°$ or $> 90°$ and both have random orientations of their particle-like electron.

The above brief synopses of the processes occurring in the beam segments are intended only as an overview of the field conditions that drive those processes. The underlying mechanisms associated with those processes are analyzed below from the perspective of LR including the energetics and dynamical forces associated with directional quantization and the measurement problem.

QuWT

3.3 SGE ANALYSIS

For the SGE the Ag beam distal to the magnet on beam segment 10 of Fig. 3.4b is effectively in a field-free region where $B_{10}=0$. The corresponding representation of the electron on the 5s orbital of an Ag atom is depicted in Fig. 3.6a as a uniform coherence wave of spin structures. The accompanying detail of that orbital in Fig. 3.6a shows a representative sampling of the spin structures all of which have a common orientation $\theta_{p-10}, \phi_{p-10}$ and a common magnitude. Of some consequence in the following analysis, the spin structure polar orientation $\theta_{p-10}<90°$. The detail sampling happens to include the singular spin structure on which the particle-like electron is located. For visual clarity, for all of the spin structures in the detail sampling, only the spinor on which particle-like electron resides is depicted. The depicted occupied spinor happens to have a polar orientation $\theta_{M-10}>90°$ but we shall see in the following that whether $\theta_{M-10}>90°$ or $<90°$ is not consequential. In contrast, an initial field-free spin structure polar orientation θ_{p-10} that is either $>90°$ or $<90°$ will be seen to be deterministically consequential. We shall follow the example of $\theta_{p-10}<90°$ here since the results of the converse $\theta_{p-10}>90°$ are readily deduced.

As the $\theta_p<90°$ 5s electron coupled to an Ag atom first enters segment 11 the field $B_{11}\approx0$ and is not substantially different from the $B_{10}=0$ throughout segment 10. Consequently, in that initial portion of segment 11 the wave representation of the electron is unchanged from that on segment 10. However, beyond that initial portion of segment 11 is a field inflection over which B_{11} substantially increases. For the SGE beam with a velocity ~10^3 m/s the sufficiency criterion for directional quantization $Q_{e-s}=6.2\times10^7$ gauss/s is estimated to occur within segment 11 approximately at y=−10 mm (where y=0 at the pole perimeter in segment 12). Since B_{11}~0 at the initial portion of segment 11, the criterion for directional quantization Q_e occurs within segment 11.

At the point Q_e is achieved, the 5s electron wave begins a condensation process as it continues along segment 11. In the transitional phase of that condensation the Fig. 3.6a uniform coherence wave of spin structures on the 5s orbital circumferentially condense toward a Gaussian distribution on the orbital as shown in Fig. 3.6b. Concurrently there is an accompanying projective condensation along the +B axis of the individual spin structures
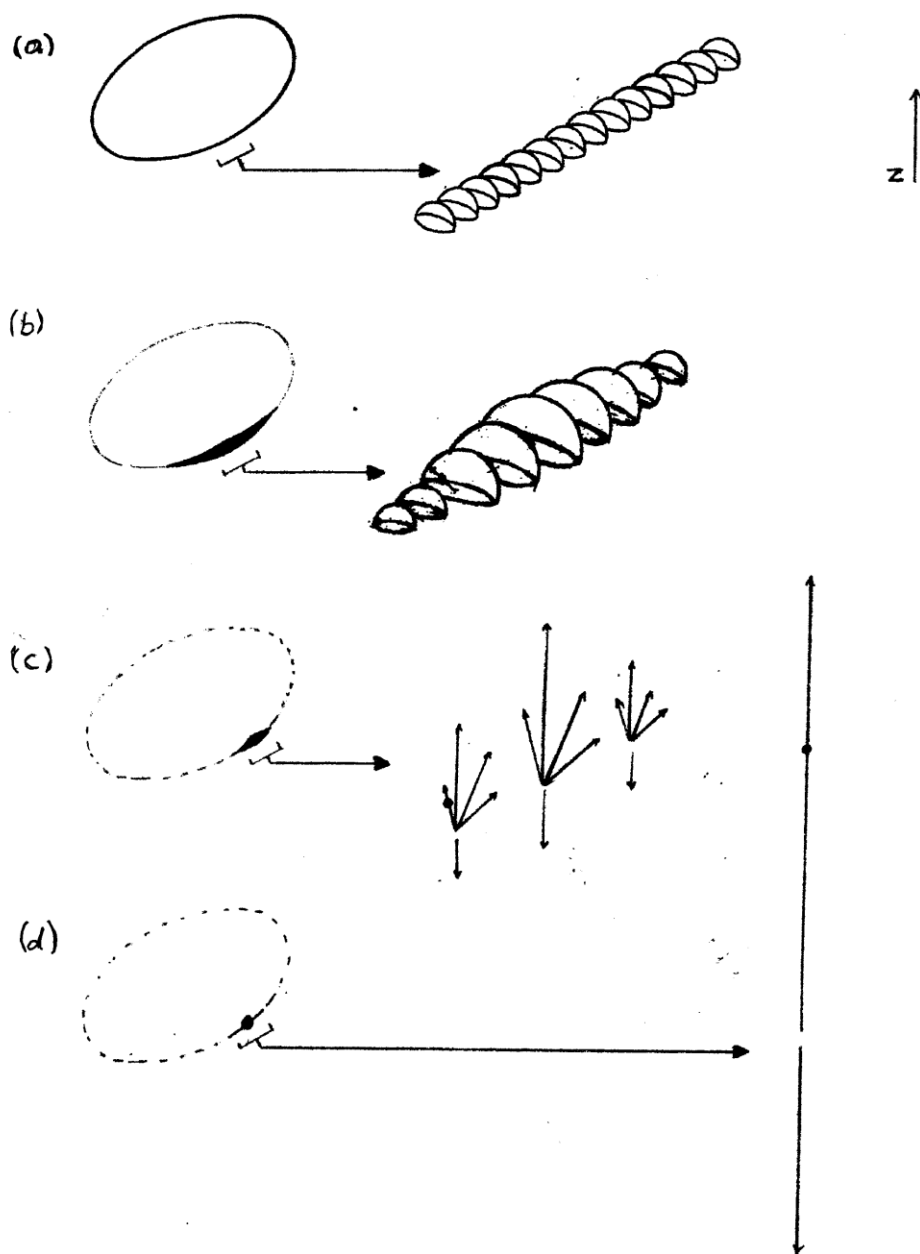
Fig. 3.6a-d. The sequence depicts electron wave samplings on the 5s orbital as the Ag atom is (a) distal to a magnetic gradient, (b-c) entering a strong magnetic gradient, and (d) fully condensed to delta-form while still in the magnetic gradient.

toward a Gaussian distribution of the constituent spinors. That projective condensation of individual spin structures along with further circumferential condensation of the spin structure Gaussian is depicted in transition in the Fig. 3.6c. detail.

These two condensation processes are shown to completion in the Fig. 6d detail as a single remaining spin structure projected to an occupied δ-form spinor along the +B axis and an empty complementary orthogonal δ-form spinor along the –B axis. The two δ-form spinors on segment 11 continue substantially unchanged onto segment 12 where the field gradient further increases. However, before proceeding further we have interest in examining mathematical representations of the segment 11 Gaussian condensation processes. And we have particular interest in examining the energetics and dynamics that drive the particle-like electron from some θ_M orientation to alignment with the +B axis at 0° since this process constitutes the essence of the directional quantization mechanism and the underlying conundrum of the measurement problem.

We proceed here with the example of with $\theta_p < 90°$ for the 5s orbital electron wave on an Ag atom. The figure depicts the concurrent processes of circumferential condensation of the coherent spin structure orbital wave to a single spin structure and the projective condensation of the individual spin structures.

3.4 PROJECTIVE CONDENSATION AND THE QUANTUM POTENTIAL

The two condensation processes can independently be examined. In the present context of LR wave packets comprised of a coherence wave of spin structures, it is of particular advantage if we model the physical characteristics of the condensations with the modulus of the wave function rather than with the entire wave function. Bohm applied this simplification of utilizing the modulus in extracting an expression for an effective quantum potential from Schrödinger's equation. We shall similarly be making use of that expression for the effective quantum potential here. We also have an immediate interest is in examining the behavior of an analytical representation of the modulus during the sudden condensation process

since the quantum potential is a function of derivatives of that modulus. Spatially, that modulus becomes highly peaked as the condensation process proceeds.

In Bohm's treatment, the complex wave function is written as

$\Psi = A \exp(iS/\hbar)$

where A is the modulus of Ψ and where A and S are real. This form of the wave function is applied to Schrödinger's one-dimensional equation

$i\hbar\partial_t\Psi = -(\hbar^2/2m)\,(\partial/\partial x)^2\Psi + V(x)\Psi$

where V(x) is a classical potential that may be present.

Bohm shows that when the field represented by ψ is treated as objectively real, the particle of mass m dynamically responds as if in a total potential

$T(x) = V(x) - (\hbar^2/2m)\,[(\partial/\partial x)^2 A]/A$

implying the existence of a "quantum potential" identified as

$U(x) = -(\hbar^2/2m)\,[(\partial/\partial x)^2 A]/A$

which notably is a function of A, the modulus of Ψ.

In the analysis of condensation we need only treat the amplitude modulus functions rather than the full wave function that is inclusive of an imaginary cofactor as applied by Bohm regarding quantum potentials. [390] The analysis of condensation will be applied here to a "spatially bounded wave," the 5s orbital of an Ag atom but first we briefly digress here to examine the properties of a common spatially unbounded Gaussian wave packet in free-space.

The one-dimensional free-space spatially unbounded Gaussian wave packet expressed as an amplitude modulus is

$A(x,t) = \pi^{-1/4}\,L(t)^{-1/2}\,\exp[-x^2/2\,L(t)^2]$

where the integral of the $A(x,t)^2$ intensity

$\int A(x,t)^2\,dx = 1$

over the limits $-\infty$ to $+\infty$ notably is an invariant of the length L(t) which is half of the characteristic Gaussian width at any time t. In the standard quantum mechanical formalism that invariance of the integral constitutes the requisite probability conservation for a process such as the rapid temporal decrease of L(t) resulting from an external perturbation, a process defined here as condensation. In the above form the presence of L(t) in the $L(t)^{-1/2}$ factor exterior to the exponential is recognized as inherently providing for the probability-conserving normalization of the integral.

In Bohm's treatment of Ψ as representing an objectively real field there is a logical expectation that the contour of the modulus must have a functional relationship in mediating the position of a particle on a wave packet based on Born's first assumption that positional probability is given by the squared modulus. [307] That expectation is explicitly excluded in PI where the non-real probabilistic particle-like and the wave-like entities are not subject to causal mechanisms that move one with respect to the other.

The force associated with a total potential T(x,t) consisting of a classical potential V(x) and the quantum potential U(x,t) is

$F(x,t)=\partial_x T(x,t)$

$\quad =\partial_x[V(x)+U(x,t)]$

$\quad =\partial_x[V(x)-(\hbar^2/2m)\,(\partial_x^2 A(x,t)/A(x,t)]$.

In the absence of a classical potential V(x) for a wave packet in free space there is a "quantum" force

$F_Q(x,t)= -(\hbar^2/2m)\,\partial_x[\partial_x^2 A(x,t)/A(x,t)]$

that preferentially drives a particle-like entity residing on the wave packet toward the peak of the wave packet at x=0. The quantum force $F_Q(x,t)$ is seen as a measure of the derivatives of the amplitude magnitude and not the absolute magnitude of the amplitude magnitude at any instantaneous time t. This force independence with respect to absolute magnitudes of the amplitude, i.e. its modulus A. This independence is evident from the form of $F_Q(x,t)$ in which the leading $\pi^{-1/4} L(t)^{-1/2}$ "scale" factor of A cancel. Conversely, the quantum force is entirely dependent upon the shape of the amplitude in coordinate space at any given time t, i.e. the shape of the Gaussian $\exp[-x^2/2\, L(t)^2]$ factor and not a multiplicative scale factor of that factor. [304]

QuWT

If that Gaussian exponential becomes more sharply peaked, e.g. as a result of a temporally diminishing L(t), $F_Q(x,t)$ increases consistent with Born's first assumption. [307]

(Parenthetically we note that Bohm's interpretation of the underlying quantum formalism achieves the same predictions as PI, including the non-local attributes of PI, but does so without abandoning objective reality. Because of the former, Bohm's representation is not testable against PI. In our presentation of LR we demonstrate an objectively real representation that is local and is testable against PI and, by extension, against Bohm's interpretation.)

However, our immediate interest here is with regard to the wave of the unpaired Ag 5s electron. In contrast to the probability on a spatially unbounded free-space wave packet, the coherence wave of uniform amplitude spin structures on the 5s orbital constitutes a spatially bounded probability. We seek here the simplest representation of the condensation of that spatially bounded probability consistent with the underlying quantum mechanical formalism.

That objective is achieved here by bounding the spin structure probability with a truncated Gaussian throughout the condensation process from a uniform circumferential distribution of equal amplitude spin structures to a singular spin structure localized on the orbital. The requisite representation begins with an orbital amplitude modulus

$$A_O(\rho,t) = \pi^{-1/4} L_N(t)^{-1/2} \exp[-\rho^2/2L(t)^2]$$

analogous to that of the free-space expression but where ρ is positional parameter along the orbital circumference. In the spatially unbounded expression $A(x,t)$ the length $L(t)$ that appears in the $\pi^{-1/4}L(t)^{-1/2}$ cofactor to the exponential provides the normalization that conserves probability. In the bounded expression $A_O(\rho,t)$ probability that would be associated with the truncated tails of the bounded Gaussian needs to be excluded in the cofactor that provides for normalization. That exclusion is achieved by setting $L_N(t) \neq L(t)$ and imposing probability conservation over the bounded Gaussian to solve for $L_N(t)$.

At t_o, prior to the onset of condensation, the circumferential 5s "wave packet" consists of a uniform amplitude bounded distribution of spin structures

QuWT

(unlike a particle wave packet in free space which is a conventional unbounded Gaussian). The initial uniform circumferential distribution of spin structures can be treated as a bounded distribution of the truncated central section of a dimensionally infinitely large Gaussian distribution since that central section is then inherently uniform in amplitude magnitude. However, probability is computed only over the bounded uniform spin structures. In that respect at $t=t_o$ we set the length parameter $L(t_o)$ to infinity, $L(t_o)=\infty$ whereupon we get the required the constancy of the exponential cofactor over all ρ, -0.5 to $+0.5$.

$\exp[-\rho^2/2\,L(t_o)^2\,]=1$

which represents a uniform amplitude modulus of the spin structures on all ρ along the orbital circumference .

At t_o we impose normalization of the integral of intensity evaluated over the unit circumference limits ±0.5

$\int A_O^2\,d\rho=1$

which sets the initial t_o probability $P=1$ and shows that

$L_N(t_o)=\pi^{-1/2}=0.56$.

In the circumferential condensation process when $L(t_o)=\infty$ decreases to finite values the distribution of spin structure intensities on the orbital is a truncated Gaussian peaked at $\rho=0$. For example at some time t_1 where $L(t_1)=0.4$, the Gaussian on the orbital is highly truncated. Since probability is conserved on that truncated Gaussian, we can readily solve for

$L_N(t_1)=0.366$.

This calculation is repeated for two more $L(t)$ values and the results are listed below together with the above two results.

For $L(t_o)=\infty$, $L_N(t_o)=0.56$.

For $L(t_1)=0.4$, $L_N(t_1)=0.37$.

When $L(t_1)=0.4$ the Gaussian width is 0.8 which is a substantial fraction of the unit circumference. As a result only the central section of a highly truncated Gaussian envelope is realized on the orbital circumference, centered at $\rho=0$. However, since that central section represents a very large

part of the total probability that would ordinarily be included in the unbounded Gaussian, the deviation of the $L_N(t_1)$ value of 0.37 from the 0.4 Gaussian length is modest.

For $L(t_2)=0.25$, $L_N(t_2)=0.247$.

When the L is reduced to 0.25 virtually all of the significant Gaussian envelope is realized on the orbital circumference and truncation is very small. In this regard the $L(t_2)=0.25$ length bounded on a unit circumference very closely approximates the analytical form for an unbounded Gaussian wave packet. This is shown by the close convergence of $L_N(t_2)=0.247$ toward the $L(t_2)=0.25$ length.

For $L(t_3)=0.15$, $L_N(t_3)=0.15$.

With $L(t_3)=0.15$ the Gaussian envelope is even more sharply peaked about the $\rho=0$ point. The extreme convergence of $L_N(t_3)=0.15$ to $L(t_3)=0.15$, with only a vanishingly small differential, further emphasizes the approximation of the analytical form to that of an unbounded Gaussian wave packet.

As L continues to decrease, the orbital amplitude modulus wave function A_O, representing a coherence wave of spin structures, effectively condenses to a single δ-form spin structure (bearing in mind that those spin structures are themselves concurrently projectively condensing).

The above LR analysis of the circumferential condensation process for the coherent spin structure wave on the orbital demonstrates that the respective wave states can be represented as Gaussian throughout that process even though they are bounded. Significantly, this analysis is consistent with the treatment of the underlying quantum formalism for condensation of unbounded Gaussians. Additionally, that LR analysis for the condensation of the coherent spin structure wave provides close analogies for the projective condensation of the individual spin structures that proceeds concurrently with the circumferential condensation. Importantly, it is from the analytical form of spin structure projective condensation that the underlying mechanism for directional quantization can be deduced.

It must be emphasized that the condensation process is the response of the initial uniform amplitude orbital wave to a sudden $\partial_t B$ that equals or exceeds Q_e and is independent of the particle-like electron that had initially resided on one of the spin structures of the orbital wave. In the condensation process of

QuWT

the orbital wave its sharply peaked modulus about $\rho=0$ provides the quantum force that progressively drives the particle-like electron toward the remaining spin structures as $L(t) \to 0$.

$$F_Q(\rho,t) = -(\hbar^2/2m_e)\, \partial_\rho[(\partial_\rho^2 A_O(\rho,t)/A_O(\rho,t)]$$

$$= -(\hbar^2/2m_e)\partial_\rho[(\partial_\rho^2 \exp(-\rho^2/2L(t)^2)/\exp(-\rho^2/2L(t)^2)]$$

$$= -\rho\hbar^2/[L(t)^4 m_e]$$

From this equation we see, not unexpectedly, that initially where $L(t_o)=\infty$, there is no net quantum force since the truncated "Gaussian" modulus is uniform over the entire orbital whereas as the condensation progresses with a decreasing $L(t)$ the quantum force toward the peak at any point ρ rapidly increases because of the $L(t)^{-4}$ dependence. This process effectively drives the particle-like electron circumferentially toward a remaining spin structure at $\rho=0$ but does so without altering the polar orientation θ_M of that electron and its magnetic moment $\boldsymbol{\mu}_e$.

Fig. 3.6a depicts a sampling of the initial spin structures on the 5s orbital at t_o. Those initial spin structures are each composed of a two-dimensional hemispherical distribution of constituent uniform-amplitude spinors bounded by the spin structure hemisphere. We again follow the example of spin structures with $\theta_p<90°$ represented on a spherical coordinate system for which the +z axis is aligned with the +B axis of the SGE magnetic field. That coordinate system is denoted as "$CS_\uparrow$" in anticipation that the condensation will occur along the +B axis, an outcome associated with a spin up state. The +z,+B alignment is consequential because when the spin structure suddenly interacts with the magnetic field the spin structure spinors condense along the constituent spinor that is aligned with B.

This condensation of spinors is independent of a particle-like electron that might be on one of the constituent spinors. An analogous condensation independence was noted in the context of empty photon waves condensing upon entry into a calcite polarizer.

$CS_\uparrow$ is utilized here because that particular coordinate system is best suited to compactly and clearly represent the projective condensation process for the $\theta_p<90°$ example. At the conclusion of this section we will show that a spherical coordinate frame $CS_\downarrow$ with +z,−B alignment together with symmetry

QuWT

considerations promptly represents the projective condensation process for the alternative example of $\theta_p > 90°$.

We continue here with a representation of spin structure condensation in the spherical coordinate system for the example of $\theta_p < 90°$. At t_o the uniform amplitude distribution of spinors on each spin structure's hemisphere can be represented as a truncated, central section of a dimensionally infinitely large two-dimensional Gaussian distribution since that central section is then inherently uniform. On this hemisphere we define a polar arc designated as β that lies entirely at an azimuthal $\phi_{p\text{-}\beta}$ and extends from the hemisphere's boundary to the hemisphere's +z axis intersection as shown in Fig. 3.7. The spinors along the β arc constitute a one-dimensional subset of the spin structure's initially uniform amplitude spinors.

At $t > t_o$ when the spin structures encounter a sudden $\partial_t B$ that equals or exceeds Q_e projective condensation is induced. For the spin structure that process relates specifically to the projection of its constituent spinors along the **B** axis orientation. As with circumferential orbital condensation, probability is similarly conserved in projective condensation and that conservation applies as well to the subset of spinors along any β arc. Accordingly, we utilize here a one-dimensional representation of projective condensation along a β arc that is analogous to that of the circumferential condensation representation for the electron's orbital. The benefits of this approach are two-fold. Firstly, the representation demonstrates that the amplitude moduli along respective β arcs are truncated Gaussians that condense to δ-form, but more importantly the representation shows that the quantum force on the "occupied" β arc, i.e. the particular arc on which a particle-like electron resides, rotates the initial orientation of the magnetic moment $\boldsymbol{\mu}_e$ from some initial θ_M to $0°$ (along the **B** axis). This rotation occurs during energy exchange between the electron with its coupled Ag atom and the magnetic field during its passage through the longitudinal gradient field $\partial_y B$.

We begin the representation of projective condensation in analogy with circumferential orbital condensation by similarly constructing an amplitude modulus A_H for a polar arc β on a spin structure hemisphere.

That objective is achieved with a spin structure "hemispherical" arc modulus

$$A_H(\eta_\beta, t, \theta_p, \phi_{p\text{-}\beta}) = \pi^{-1/4} \ell_N(t, \theta_p, \phi_{p\text{-}\beta})^{-1/2} \exp[-\eta_\beta^2 / 2\ell(t)^2]$$

defined along a polar arc β lying in an azimuthal $\phi_{p\text{-}\beta}$ plane on the spin structure as shown in Fig. 3.7. On the spin structure hemispherical surfaces η_β is defined as a positional quantity $\eta_\beta = \theta$ where an arbitrary unit radius serves purely as a mathematical intermediary to give η_β the dimensions of length, parameterized by the positional polar orientation θ. The parameter η is subscripted by β because hemispherical boundaries for respective polar arcs are dependent upon $\phi_{p\text{-}\beta}$ and θ_p (except in the singular case of $\theta_p = 0°$). That dependency also necessitates the functional dependence of A_H and ℓ_N on θ_p and $\phi_{p\text{-}\beta}$. That angular dependency is not applicable to $\ell(t)$ which is a monotonically decreasing function of time representing the condensation response of the spin structure's spinors to a sudden change in magnetic field.
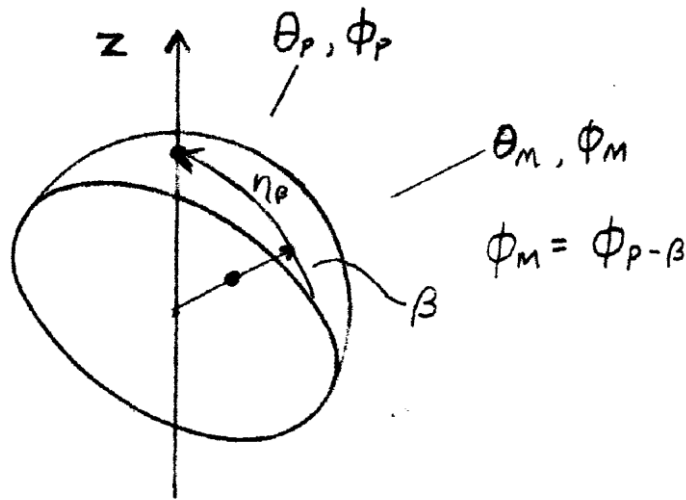

*Fig. 3.7. Detail showing the polar arc β on the occupied spin structure long which the relevant forces drive the occupied spinor into alignment with **B**.*

The spin structure has an orientation θ_p, ϕ_p. Relative to the +B axis, which is equivalent to the +z axis, the physical orientation of the pole's azimuthal ϕ_p can be arbitrarily assigned unlike the polar orientation θ_p. For A_H, the lengths $\ell_N(t, \theta_p, \phi_{p\text{-}\beta})$ and $\ell(t)$ are the analogs of the lengths $L_N(t)$ and $L(t)$ associated with the orbital amplitude modulus A_O expression.

As noted above, $A_H(\eta_\beta, t, \theta_p, \phi_{p\text{-}\beta})$ identifies the circumferential amplitude magnitude of the constituent spinors along a polar arc on the hemispherical spin structure as shown in Fig. 3.7 where that arc lies in a plane at some azimuthal $\phi_{p\text{-}\beta}$. Before projective condensation begins at a time t_o the length $\ell(t_o) = \infty$ resulting in a uniform amplitude of constituent spinors given by

QuWT

$A_H(\eta_\beta, t_o, \theta_p, \phi_{p-\beta}) = \pi^{-1/4} \ell_N(t_o, \theta_p, \phi_{p-\beta})^{-1/2}$

since the un-normalized Gaussian exponential co-factor of A_H,

$\exp(-\eta_\beta{}^2/2 \, \ell(t_o)^2) = 1$.

Concurrently, the length $\ell_N(t_o, \theta_p, \phi_{p-\beta})$ is constrained to a well-defined, finite value as it provides for the necessary probability normalization of the uniform amplitude spinors along the Fig. 3.6a β polar arc at time t_o.

Because of the bounded distribution of those inclusive β arc spinors on the hemispherical surface, $\ell_N(t, \theta_p, \phi_{p-\beta}) \neq \ell(t)$ at any time t in analogy to $L_N(t)$ and $L(t)$ for A_O. Beyond t_o the spin structures evolve through a transitional projective condensation in which $\ell(t)$ decreases in representation of the distribution of the amplitude moduli of spinors on a β arc sharply peaking along +B. Concurrently, the quantity $\ell_N(t, \theta_p, \phi_{p-\beta})^{-1/2}$ serves as a progressively increasing compensating normalization scaling factor for the spinor amplitude moduli along any selected β polar arc. Normalization imposes a well-defined constraint on the value of ℓ_N during the transitional phases of condensation.

With regard to ℓ_N there is an important distinction between the orbital condensation of the coherent spin structure wave associated with $A_O(\rho, t)$ and the projective condensation associated with $A_H(\eta_\beta, t, \theta_p, \phi_{p-\beta})$. As $t_o \rightarrow t$ there is an apparent loss of probability associated with the integration of $A_H{}^2$ over all constituent spinors of the progressively deforming spin structure. This loss is attributable to the spinor algebra projection of a physically contiguous, orthogonal spinor along the –B axis that is extracted from the projectively condensing spinors as shown in Fig. 3.6c. That loss is taken into account in the $\ell_N(t, \theta_p, \phi_{p-\beta})$ value of $A_H(\eta_\beta, t, \theta_p, \phi_{p-\beta})$ but does not affect $\ell(t)$.

Fig. 6d depicts the sudden process of spatial condensation and projective condensation to completion. The spatial condensation has effectively reduced the coherence wave packet of spin structures to a single spin structure which itself has projectively condensed to a single δ-form spinor. From spinor algebra, the relative probability of that δ-form (occupied) spinor, identified as "$\mathbf{s}_u$" in Fig. 3.6d, is

$P = \cos^2(\theta_p /2)$.

Concurrently, from spinor algebra the condensation process also generates a complementary orthogonal δ-form (empty) spinor with a relative probability

$P = \sin^2(\theta_p/2)$

showing that total probability is conserved. The occupied δ-form spinor s_U and the empty δ-form spinor s_d are initially contiguous. Our immediate focus in this section is a demonstration that the amplitude modulus along a β arc of the condensing occupied spin structure continues to be Gaussian despite the progressive loss of probability that reaches $P = \sin^2(\theta_p/2)$ on the complementary empty δ-form spinor s_d. Accordingly, we continue with that focus here and defer a consideration of that empty δ-form spinor to a later point in this section.

The $P = \cos^2(\theta_p/2)$ endpoint of probability on the occupied δ-form is recognized as a further mathematical constraint on the transitional values of $\ell_N(t,\theta_p,\phi_{p\text{-}\beta})$ during projective condensation. It can readily be appreciated that the form of the amplitude magnitude $A_H(\eta_\beta,t,\theta_p,\phi_{p\text{-}\beta})$ already provides for a Gaussian intensity A_H^2 along any polar β arc at any instant in time t during the projective condensation process such as that shown in Fig. 3.6c.

A complete functional value of that intensity requires an analytical expression of the probability scaling length $\ell_N(t,\theta_p,\phi_{p\text{-}\beta})$ for any time t. The analysis to this point demonstrates that ℓ_N is a well-defined, mathematically constrained quantity from which such an analytical expression can reasonably be constructed, albeit with substantially greater complexity than that for $L_N(t)$. However, a primary focus here is in calculating the quantum force associated with the condensing amplitude modulus A_H. In that calculation an analytical expression for the probability scaling length $\ell_N(t,\theta_p,\phi_{p\text{-}\beta})$ is not needed because, as was the case for $L_N(t)$, the probability scaling length quantities cancel in the calculation of quantum force.

It must be emphasized that the condensation process is caused by the sudden encounter of the wave with a magnetic field in satisfaction of the Q_e criterion. That process occurs independently of the presence of the particle-like electron on the wave. If there is a particle-like electron residing on the wave, e.g. at some initial orientation on a spinor at θ_M,ϕ_M, quantum forces that occur during the transitional condensation process move the electron to the δ-form spinor forming along the +B axis. It is the re-orientation of the electron spin that constitutes directional quantization. As the projective

condensation process proceeds, the relevant force is in the azimuthal plane that includes the electron-occupied spinor along a β arc. Consequently $\phi_{p\text{-}\beta}=\phi_M$.

3.5 QUANTUM AND CLASSICAL FORCES IN PROJECTIVE CONDENSATION

The quantum force F_{uQ} together with the relevant classical magnetic force F_{uM} is the total force F_u. Forces for the present $\theta_p<90°$ example are subscripted by "u" in anticipation that the measurement result is spin "up". Then the total force

$F_u(\eta_\beta,t,\theta_p,\phi_{p\text{-}\beta})=\partial(V+U)/\partial\eta_\beta$

$\quad=\partial\{\boldsymbol{\mu}_e\bullet\mathbf{B}(t)-(\hbar^2/2m_e)\,[(\partial^2 A_H/\partial\eta_\beta\,\partial\eta_\beta)/A_H]\}/\partial\eta_\beta$

$\quad=\partial\{\mu_e\,B(t)\,\cos\eta_\beta-(\hbar^2/2m_e)\,\{[\partial^2\exp(-\eta_\beta^2/2\,\ell^2)/\partial\eta_\beta\,\partial\eta_\beta]/\exp(-\eta_\beta^2/2\,\ell^2)\}/\partial\eta_\beta$

$\quad=-\mu_e B(t)\,\sin\eta_\beta-\eta_\beta\hbar^2/\ell^4 m_e$

$\quad= F_{uM}+ F_{uQ}$

The classical magnetic potential $V=\boldsymbol{\mu}_e\bullet\mathbf{B}(t)$ is associated with the electron's magnetic moment at some time t when the Ag atom to which the electron is coupled is located in a field B(t) and $\boldsymbol{\mu}_e$ is at some $\theta=\eta_\beta$ on the unit radius of the spin structure. $F_u(\eta_\beta,t,\theta_p,\phi_{p\text{-}\beta})$ expresses the sum of the classical magnetic force F_{uM} and quantum force F_{uQ} acting on the particle-like electron that resides on a spin structure. The force is applicable to an objectively real incident spin structure wave for which $\theta_p<90°$ where both the classical and the quantum potentials contribute negatively signed forces that drive the particle-like electron to the $+\mathbf{B}$ axis where $\eta_\beta=0$ and $\theta=0°$ resulting in a "spin up" measurement.

This result in which electron is driven to +B where $\theta=0°$ occurs even if the initial polar orientation of the electron is at some $\theta_M>90°$. This outcome is deterministically set by the condition $\theta_p<90°$ which dictates that the Gaussian modulus condensation, from which the quantum force is derived, is along +B.

QuWT

The $F_u(\eta_\beta,t,\theta_p,\phi_{p-\beta})$ expression for the force is independent of the probability scaling coefficient ℓ_N. An analogous independence with respect to absolute magnitude was noted above in conjunction with the quantum force associated with the circumferential orbital condensation. Both of those condensations involve bounded Gaussians. In [390] Bohm had observed that because of the functional dependence of the quantum force on the amplitude modulus, the quantum force is inherently independent of the absolute magnitude of that amplitude. In the present analysis we have an example of that independence specifically relating to the probability scaling factors associated with bounded Gaussian amplitudes.

As we noted earlier the analysis for projective condensation has proceeded with the example of $\theta_p<90°$. That analysis utilizes the spherical coordinate system $CS_\uparrow$ to advantage since the spin up spinor projective condensation occurs along the +B axis which is aligned with the +z axis in $CS_\uparrow$. As a result of using $CS_\uparrow$, transitional Gaussians are conveniently centered at the β arc origin $\eta_\beta=0$, derived forces direct the particle-like electron toward that origin and the associated mathematical representations of those quantities are rendered in their simplest, most transparent form.

The analysis of projective condensation for the alternative example of $\theta_p>90°$ can also be analyzed using $CS_\uparrow$. However, because the spin down projective condensation then occurs along the −B axis, the resultant mathematical representations would not be expressed in an optimal form. That deficiency is most expeditiously achieved by switching to an inverted spherical coordinate system $CS_\downarrow$ in which +z and −B are aligned. The $\theta_p>90°$ condition in $CS_\uparrow$ becomes $\theta_p<90°$ in $CS_\downarrow$ and symmetry considerations immediately allow us to write the force that drives the particle-like electron toward the −B axis where $\eta_\beta=0$. That force expressed in $CS_\downarrow$ is

$F_d(\eta_\beta,t,\theta_p,\phi_{p-\beta})=\partial(V+U)\diagup\partial\eta_\beta$

$\quad=\partial\{-\boldsymbol{\mu}_e\boldsymbol{\cdot}\mathbf{B}(t)-(\hbar^2/2m_e)\,[(\partial^2 A_H/\partial\eta_\beta\,\partial\eta_\beta)/A_H]\}\diagup\partial\eta_\beta$

$\quad=\partial\{-\mu_e\,B(t)\cos\eta_\beta-(\hbar^2/2m_e)\,\{[\partial^2\exp(-\eta_\beta^2\diagup 2\,\ell^2)/\partial\eta_\beta\,\partial\eta_\beta]\diagup\exp(-\,\eta_\beta^2/2\,\ell^2\,)\}\}\diagup\partial\eta_\beta$

$\quad=\mu_e B(t)\sin\eta_\beta-\eta_\beta\hbar^2\diagup\ell^4 m_e$

$\quad= F_{dM} + F_{dQ}$

QuWT

The above total force F_d expressed in $CS_\downarrow$ results in a spin down measurement relative to **B**. The force F_d is identical to the F_u force expressed in $CS_\uparrow$ that results in a spin up measurement aside from a necessary change of sign in the former for the field B. That change in sign causes the F_{dM} classical magnetic contribution of the force arising from the V potential to oppose the negatively signed F_{dQ} quantum force that drives the particle-like electron toward the −B axis. Initially at some time t_1 shortly after t_o, $\ell(t_1)$ is still relatively large and the positive classical force dominates resulting in a net positive force that drives the electron away from the −B axis. However, $\ell(t)$ continues to decrease beyond t_1 during the condensation process. Since the magnitude of the negative quantum force term is proportional to $\ell(t)^{-4}$, the initially positive net force rapidly transitions to a progressively larger negative net force that drives the electron to the −B axis, measured as a spin down event.

The forces that drive the electron toward directional quantization are depicted in Fig's. 3.8a-d. Fig. 3.8a shows the quantum forces F_{uQ} and F_{dQ} in their respective $CS_\uparrow$ and $CS_\downarrow$ at progressively increasing times t_1, t_2, and t_3 during projective condensation. The negative quantum forces drive the electron along the β-arc parameter $\eta_\beta \rightarrow 0$ corresponding to directional quantization. The magnitudes of those quantum forces increase over time as the Gaussian wave becomes more sharply peaked. The classical magnetic forces F_{uM} and F_{dM}, shown in Fig. 3.8b in their respective $CS_\uparrow$ and $CS_\downarrow$, are oppositely signed. Figs. 3.8c and 3.8d respectively depict the net forces F_u and F_d at t_3. Because of the positive value of the F_{dM} contribution to the net force, the magnitude of F_u exceeds that of F_d along η_β. Nevertheless, in both cases the outcome of directional quantization is reached within segment 11 well before the electron enters the transverse gradient region of the SGE magnet in segment 14 that produces the deflection of the electron and its coupled Ag atom.

The above examination of the forces that produce directional quantization does not address the associated energy transfers. In the early analysis of the SGE by Einstein and Ehrenfest, [382] they considered known classical processes that would emit or absorb the requisite energy that would yield quantum state transitions to parallel or antiparallel alignments as the Ag atom traversed the magnet's high transverse gradient field (segment 14 in Fig. 3.4). [383] Their conclusion then that known classical processes did not

provide a basis for the requisite energy has substantially endured and has contributed to the general acceptance of the probabilistic interpretation, PI. [384]

In our examination here for the LR basis of that requisite energy we note that the transfers necessarily occur outside of the perimeter of the SGE magnet poles in beam segment 11 on Fig. 3.4 and not on segment 14. As the Ag
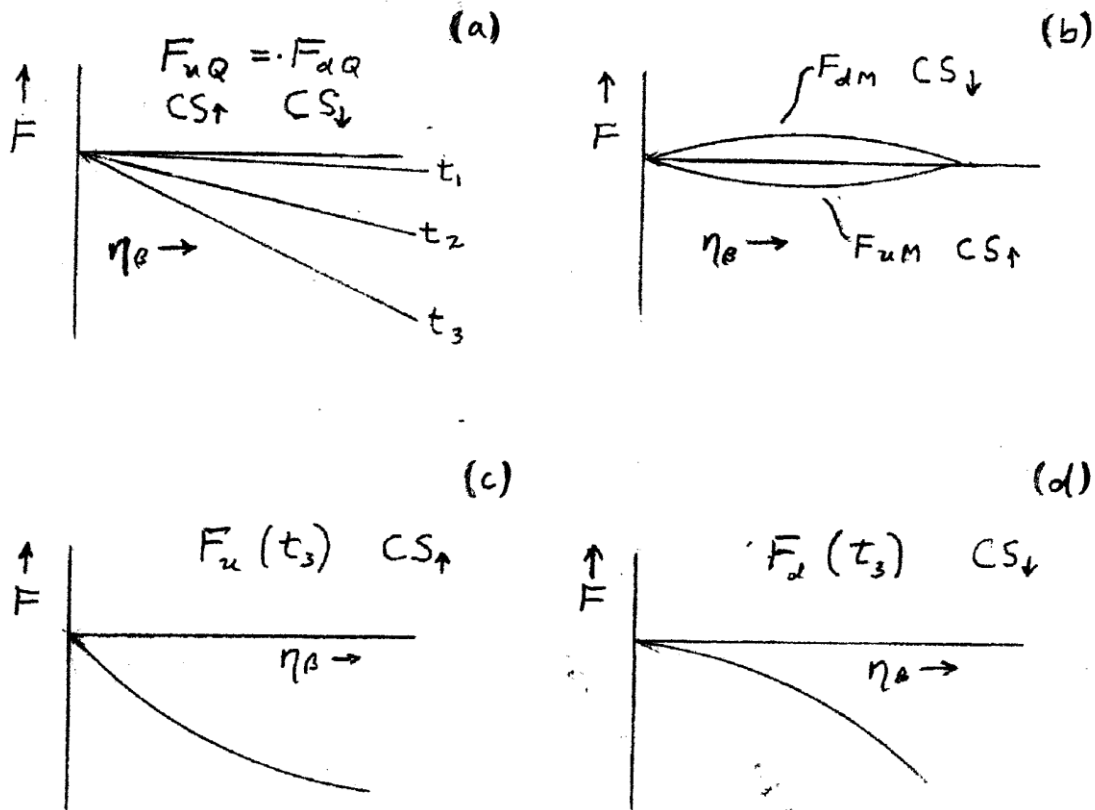
Fig's. 3.8a-d. (a) qualitatively shows the quantum force acting upon the electron for three times t_1, t_2, and t_3 representing temporal points of the spin structure's progression to a highly singular probability distribution at t_3. This force is independent of the spin state. (b) is the classical electromagnetic force which is spin dependent. (c) and (d) depict the two resultant forces for spin up and spin down that differ in detail because of the spin dependency but not in outcome.

atom traverses segment 11 the B field increases from some negligible B value to B~10^3 Gauss which very approximately is inclusive of the exterior inflection region of the longitudinal fringe field gradient. Within that segment the sufficiency criterion of 6.2×10^7 gauss/s is achieved at B~600 gauss where $\partial_y B = -63$ gauss/mm. For the randomly oriented incident Ag atoms the polar orientation θ_p of the electrons spin structures and the polar orientation θ_M of the spinor on which the electron resides are similarly random.

3.6 ENERGETICS OF DIRECTIONAL QUANTIZATION

For the spin up example of $\theta_p < 90°$ on $CS_\uparrow$ the initial, random θ_M for the electron ranges from 0° (along +B) to almost 180°, corresponding respectively to the electron being initially directionally quantized to being almost anti-aligned with +B. Since the $\boldsymbol{\mu}_e$ orientation is opposite to that of the electron, the latter extreme corresponds to a $2\mu_e$ change in magnetic moment along +B following directional quantization. On average however the change in magnetic moment along +B is somewhat less than μ_e so, to order of magnitude, that change is approximated as $\Delta\mu_e \sim -\mu_e$, effectively from giving the z component of $\boldsymbol{\mu}_e$ a rotation from 90° (where it is 0) to 180° (where it is $-\mu_e$). Then, in the neighborhood of B~600 gauss the directional quantization energy

$$\Delta E_{DQ} \sim \Delta\mu_e B \sim -10^{-20} \cdot 600 \sim -6 \times 10^{-18} \, erg.$$

In this directional quantization process for the example of $\theta_p < 90°$ on $CS_\uparrow$ the energy change ΔE_{DQ} is negative since the electron is in a lower energy state as a result of the anti-alignment of its magnetic moment $\boldsymbol{\mu}_e$ and the magnetic field **B**. The negative ΔE_{DQ} represents an energy lost by the electron Ag atom system during the spin up directional quantization process.

Once directional quantization is promptly achieved within segment 11 at B~600 gauss it is of complementary relevance to also evaluate the dynamics of the electron with its coupled Ag atom as it traverses the longitudinal gradient that extends over segments 11, 12, and 13. The electron achieves directional quantization within segment 11 and remains directionally quantized as long as there are no forces to perturb it from that condition. Consequently, the electron is directionally quantized over the remainder of

segment 11 and all of segments 12 and 13. The change in field is $\Delta B_{11\to13}\sim10^4$ gauss. Then over segments $11\to13$ there is a change in energy

$\Delta E_{KE}\sim -\mu_e\,\Delta B_{11\to13} \sim -10^{-20}\cdot10^4 \sim -10^{-16}$ erg.

The quantity ΔE_{KE} is negative because the energy of the electron Ag atom system is progressively reduced as the system traverses segments $11\to13$. This reduction occurs since the initial low energy state of the anti-aligned $\boldsymbol{\mu_e}$ and **B** is further reduced as the magnitude of **B** increases. In this process the negative quantity ΔE_{KE} represents energy lost by the electron Ag atom system during the traversal of segments $11\to13$. The manifestation of this loss is a reduction in the kinetic energy of that system. The initial kinetic energy of the electron Ag atom system

$E_{KE}=M_{Ag}v^2/2=1.8\mathrm{x}10^{-22}\cdot(10^5)^2/2 \approx 10^{-12}$ erg

is diminished by $\sim10^{-16}$ erg, representing a 0.01% reduction in kinetic energy.

The instructive benefit of examining the above kinetic energy loss ΔE_{KE} alongside the directional quantization energy loss ΔE_{DQ} is that both processes have a common origin, the interaction of the electron Ag atom system with the longitudinal gradient magnetic field. Effectively this interaction is a collision of that system with the gradient field. Both processes similarly constitute energy emissions of the system to the field for the presently considered spin up case, $\theta_p<90°$ on $CS_\uparrow$. For the alternative spin down case $\theta_p>90°$ on $CS_\uparrow$ (equivalently, $\theta_p<90°$ on $CS_\downarrow$), symmetry considerations immediately show that both of those energy transfers are respectively the same magnitude but opposite in sign meaning that both processes constitute energy absorptions of the system from the field.

It can readily be appreciated that from the perspective of LR the directional quantization process goes to completion in beam segment 11 well before the perimeter of the SGE magnet poles is entered.

3.7 EMPTY WAVES AND PROGRESSION OF WAVE STATES ON BEAM SEGMENTS

Before we continue with further consideration of the electron Ag atom system as it progresses through the remaining segments, we first consider an ancillary event that occurs during the segment 11 projective condensation in which an empty wave entity is split off of the occupied 5s orbital wave of the

QuWT

Ag atom. From the perspective of LR this event is analogous to the splitting of a photon into an occupied δ-form wave packet and an empty δ-form wave packet as the photon enters a birefringent material such as calcite.

In anticipation of considering multiple propagating entities arising from splitting events, we separately symbolize those entities by representing them with their respective wave functions using abbreviated arguments of the relevant LR parameters. On beam segment 10 for the unpaired 5s electron of the Ag atom

$$\Psi_{e\text{-}10}=\Psi_{e\text{-}10}(\theta_{p\text{-}10},\theta_{M\text{-}10},P_{10})$$

suffices in that regard. For the present example where the pole of the 5s spin structures have a polar $\theta_{p\text{-}10}<90°$ on segment 10, the electron's orientation with a polar $\theta_{M\text{-}10}$ must be on the hemisphere defined by $\theta_{p\text{-}10}$ at some azimuthal $\varphi_{p\text{-}10}$, and $P=1$.

Fig. 3.9 is an exaggerated depiction of the beam path segments, both deflected and undeflected. $\Psi_{e\text{-}10}$ is represented as an "e" on segment 10.
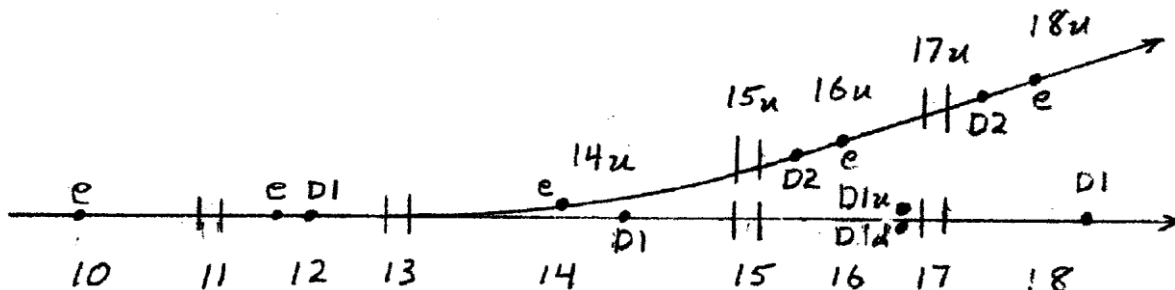
Fig. 3.9 Deflected and undeflected beam path segments in SGE for an incident polar orientation <90°.

As the transitional segment 11 is first entered, only a very weak longitudinal gradient is present and the initial wave function

$$\Psi_{e\text{-}11i}(\theta_{p\text{-}11i},\theta_{M\text{-}11i},P_{11i})=\Psi_{e\text{-}11i}(\theta_{p\text{-}10},\theta_{M\text{-}10},P_{10})$$

is unchanged from that of $\Psi_{e\text{-}10}$. However, as the electron Ag atom system has a sudden encounter with the high longitudinal gradient $\partial_y B$ within segment 11, the Q_e criterion is reached and exceeded. A rapid condensation

QuWT

process produces an occupied δ-form spinor oriented along 0°. The notation θ_δ on any segment specifies the orientation of the δ-form spinor generated by a condensation process and represents either 0° or 180°. Since $\theta_{p-11i}=\theta_{p-10}<90°$, $\theta_{\delta-11f}=0°$. The final wave function within segment 11 is

$$\Psi_{e-11f}(\theta_{\delta-11f},P_{11f})=\Psi_{e-11f}(0°,\cos^2(\theta_{p-10}/2)).$$

For the present example of an incident $\theta_{p-10}<90°$ on segment 10 we noted above that during the projective condensation on segment 11 the occupied δ-form spinor aligned to +B at 0° retains a $P_{11f}=\cos^2(\theta_{p-10}/2)$ fraction of the P=1 probability (integrated wave intensity) that had been on the 5s orbital wave of $\Psi_e(10,\theta_{p-10})$. That leaves a probability on Ψ_{e-11f} of $P_{11f}=\cos^2(\theta_{p-10}/2)$.

The remaining $P=\sin^2(\theta_p/2)$ fraction of the incident $P_{10}=1$ probability is projected onto a complementary, orthogonal empty δ-form spinor aligned to –B. The resultant empty δ-form spinor that exits segment 11 is identified as

$$\Psi_{D1-11f}(\theta_{D1-\delta-11f},P_{D1-11f})=\Psi_{D1-11f}(180°,\sin^2(\theta_{p-10}/2)).$$

DARK WAVE: The "D1" subscript on Ψ_{D1-11f} signifies that this entity is an empty "dark" wave and that it is the first one generated in the process of the transit of the Ag atom through the SGE magnet. The quantities $\theta_{D1-\delta-11f}$ and P_{D1-11f} are subscripted by D1 to distinguish them from the respective quantities $\theta_{\delta-11f}$ and P_{11f} on Ψ_{e-f}. The D1 empty wave is given the alternative assignation of a dark wave since a typical particle detector would not readily measure its impact.

The oppositely aligned δ-forms are momentarily physically contiguous at the completion of projective condensation within segment 11 however the longitudinal gradient decelerates the occupied δ−form spinor and its coupled Ag atom with respect to the dark δ−form spinor which continues as a separated, free entity at substantially the same velocity as that of incident Ag atom on the initial segment 10. The D1 dark wave has the same velocity as that of the electron Ag atom system at the completion of projective condensation.

The dark wave, moving at some velocity v<c, constitutes a mass-bearing entity. That mass is proportional to the probability P associated with the dark wave. The wave-associated mass is a property independent of the presence or absence of a particle-like entity. For example, the segment 10 initially

QuWT

occupied wave with P=1 has some mass m_{e-w} that is much less than the mass m_e associated with the electron, i.e.

$m_{e-w} \ll m_e$.

A dark wave with a probability $P=\sin^2(\theta_p/2)$ extracted from that initial occupied electron wave unit probability has a mass

$m_{D-w}=P\ m_{e-w}$

   $=\sin^2(\theta_p/2)\ m_{e-w}$

After that extraction

$m_e - m_{D-w} = m_e - \sin^2(\theta_p/2)\ m_{e-w}$

is the remaining mass associated with the electron.)

OCCUPIED WAVE: We continue here with a detailed examination of the electron Ag atom system as it exits segment 11 as an occupied δ-form spinor along +B and enters the subsequent segments. For segment 12, where the longitudinal gradient increases beyond that of segment 11, Q_e is exceeded. The continuous $\partial_t B$ over segment 12 can be modeled as repetitions of sudden ΔB increments over short Δt increments. These repetitions maintain the occupied δ-form along +B and the magnetic moment $\boldsymbol{\mu}_e$ along −B. Consequently,

$\Psi_{e-12}(\theta_{\delta-12},P_{12})=\Psi_{e-11f}(\theta_{\delta-11f},P_{11f})$

$\qquad\qquad =\Psi_{e-12}(0°,\cos^2(\theta_{p-10}/2))$.

DARK WAVE: Concurrently, the dark δ-form spinor $\Psi_{D1-11f}(180°,\sin^2(\theta_{p-10}/2))$ exiting segment 11 enters segment 12, unchanged as $\Psi_{D1-12}(180°,\sin^2(\theta_{p-10}/2))$, where it is identified as "D1" on segment 12 in the exaggerated Fig. 3.9 depiction of the respective trajectories through the SGE magnet. On segment 12 an "e", retarded relative to D1, represents the occupied δ-form of the Ψ_{e-12} electron Ag atom system Ψ_{e-12}. The retardation separation increases as the two entities traverse the remainder of segment 11, all of segment 12 and part of segment 13 because of the continued longitudinal gradient deceleration of the electron Ag atom system. The δ-form is maintained for both entities because Q_e is continuously exceeded over those same segment regions.)

QuWT

The electron Ag atom system enters segment 13 as

$\Psi_{e\text{-}13i}(\theta_{\delta\text{-}12},P_{12})=\Psi_{e\text{-}12}$

$\qquad\qquad =\Psi_{e\text{-}13i}(0°,\cos^2(\theta_{p\text{-}10}/2)).$

and passes through an inflection of the field where the longitudinal gradient suddenly decreases. At some point in this segment $\partial_t B$ falls below Q_e and the occupied δ-form spinor begins to evolve back to a uniform amplitude coherent spin structure wave over the 5s orbital. This evolution is an emission process of the δ-form spinor in which the $\theta_{p\text{-}13f}$ for the orbital wave spin structures is the polar orientation of a random member of a 0° polarization ensemble. Nevertheless, that new $\theta_{p\text{-}13f}<90°$ as was the incident value of $\theta_{p\text{-}10}$ on segment 10. The continued presence of the very substantial B along 0° ensures that the magnetic moment $\boldsymbol{\mu}_e$ remains along −B during the disruption of spinors transitionally evolving from δ-form back to a uniform amplitude coherence wave of spin structures on the 5s orbital, but with $P=\cos^2(\theta_{p\text{-}10}/2)$, as the end of segment 13 is reached. That final wave function on segment 13 is represented as

$\Psi_{e\text{-}13f}=\Psi_{e\text{-}13f}(\theta_{p\text{-}13f},\theta_{M\text{-}13f},P_{13f})$

$\qquad =\Psi_{e\text{-}13f}(\theta_{p\text{-}13f},0°,\cos^2(\theta_{p\text{-}10}/2)).$

DARK WAVE: The free D1 empty δ-form spinor enters segment 13 in its segment 12 state.

$\Psi_{D1\text{-}13i}=\Psi_{D1\text{-}12}$

$\qquad =\Psi_{D1\text{-}13i}(180°,\sin^2(\theta_{p\text{-}10}/2))$

and evolves to a free, Gaussian empty wave packet

$\Psi_{D1\text{-}13f}(\theta_{D1\text{-}p\text{-}13f},P_{D1\text{-}13f})=\Psi_{D1\text{-}13f}(\theta_{D1\text{-}p\text{-}13f},\sin^2(\theta_{p\text{-}10}/2))$

after passing through a point at which $\partial_t B<Q_e$. This evolution is an emission process of the D1 δ-form spinor in which the $\theta_{D1\text{-}p\text{-}13f}>90°$ for the orbital wave spin structures is the polar orientation of a random member of a 180° polarization ensemble. Probability is maintained in the emission process giving

$P_{D1\text{-}13f}=\sin^2(\theta_{p\text{-}10}/2)$

for the free empty Gaussian coherence wave of spin structures.

QuWT

OCCUPIED WAVE: As the electron Ag atom system enters segment 14 the 5s orbital wave continues throughout that segment as the uniform amplitude coherence wave of spin structures that exited segment 13 with

$\Psi_{e\text{-}14u}=\Psi_{e\text{-}13f}$

$\quad=\Psi_{e\text{-}14u}(\theta_{p\text{-}13f},0°,\cos^2(\theta_{p\text{-}10}/2)).$

From a measurement perspective that wave of spin structures is still in a directionally quantized spin up state since the particle-like electron resides on a spinor aligned with +B and $\boldsymbol{\mu}_e$ is then aligned along –B. On segment 14 there is no consequential longitudinal gradient and $B(y)\approx10^4$ gauss. The apex ridge geometry of the "lower" pole of the magnet produces a transverse gradient $\partial_z B\approx-10^5$ gauss/cm on the segment 14 beam path. In the SGE there is an observed $\Delta z=+0.01$ cm deflection of the electron Ag atom system after traversing the ~3 cm segment 14 beam path. That upwardly deflected path is identified as segment 14u to differentiate it from segment 14 which is a rectilinear extension of the previous segments. Over the length of segment 14 the field along +z has changes by

$\Delta B=\Delta z\ \partial_z B$

$\quad\approx+0.01$ cm $(-10^5$ gauss/cm$)$

$\quad\approx-10^3$ gauss.

At the beginning of the segment 14u path the electron Ag system is in a low energy state

$E_i=-\mu_e\ B_i$

$\quad\approx-10^{-20}\ 10^4$

$\quad\approx-10^{-16}$ erg

because of the anti-alignment of $\boldsymbol{\mu}_e$ and **B**.

At the end of segment 14u the energy of the system is

$E_f=-\mu_e\ B_f$

$\quad=-\mu_e\ (B_i+\Delta B)$

$\quad\approx-10^{-20}\ (10^4-10^3)$ erg

giving an energy change

QuWT

$E_f - E_i \approx +10^{-17}$ erg.

This positive result represents an energy increase of the system unlike the two energy losses incurred in segments 11→13. Consequently, the system absorbs 10^{-17} erg from the SGE magnetic field over the segment 14u traversal. That energy is physically manifested as a momentum along +z of the system.

It is of some interest to observe that the 10^{-17} erg energy gain associated with the deflection, that constitutes the basis for SGE measurement of directional quantization, is smaller by an order of magnitude than the kinetic energy loss of 10^{-16} erg that the system incurred as it traversed the longitudinal gradient in segments 11→13. However, from an experimental point of view the longitudinal gradient is of little utility in demonstrating directional quantization in the original SGE for several reasons. The directionally quantized electron Ag atom systems emerging from segment 13 are not physically separated on different trajectories so energy measurement would have to be employed to differentially distinguish the differing kinetic energies of the spin up and spin down states. Available detector energy resolution of 0.01% was (and still is) not achievable and the energy distribution of the incident Ag atoms would in any case totally obscure the 0.01% longitudinally induced energy increments. And finally, even if adequate energy discrimination were possible, the lack of physical separation of the spin states would require a very low beam density to permit individual energy measurement of each Ag atom.

Rabi, however, was able to demonstrate directional quantization with a longitudinal gradient by the insight that an oblique trajectory of the beam through that gradient would translate the resultant energy differential into a measurable deflection that provides the beam separation characteristic of directional quantization. [385]

In the following the respective dispositions of the dark waves and the occupied waves are separately and alternately tracked:

DARK WAVE: Over the course of segment 14 the free empty Gaussian wave packet represented by

$\Psi_{D1-14} = \Psi_{D1-13f}$

$\quad = \Psi_{D1-14}(\theta_{D1-p-13f}, \sin^2(\theta_{p-10}/2))$

QuWT

continues to further separate along the y axis relative to the electron Ag atom system on segment 14u as shown in Fig. 9 despite the lack of a $\partial_y B$ gradient retarding the latter. This further separation occurs because of the momentum loss already incurred by the electron Ag atom system in previous segments where a significant $\partial_y B$ was present.

OCCUPIED WAVE: As the electron Ag atom system exits segment 14u and first enters the transitional segment 15u the wave function is initially

$\Psi_{e\text{-}15u\,i}=\Psi_{e\text{-}14u}$.

Transitional segment 15u is inclusive of an inflection of the magnetic field over which the relatively negligible $\partial_y B$ gradient suddenly changes to a large negative $\partial_y B$ while conversely the high transverse gradient $\partial_z B$ decreases to a negligible value. As a consequence, in the sudden encounter of the uniform amplitude 5s coherence wave of spin structures with the segment 15u $\partial_y B$ gradient, the Q_e directional quantization criterion is reached and exceeded causing the wave to undergo a condensation process closely analogous to that in transitional segment 11. In that process the probability of the occupied δ-form spinor is reduced by a factor of $\cos^2(\theta_{p\text{-}13f}/2)$ as a result of the segment 15u projective condensation. That leaves a probability

$P=\cos^2(\theta_{p\text{-}13f}/2)\cdot\cos^2(\theta_{p\text{-}10}/2)$

on the final occupied δ-form

$\Psi_{e\text{-}15u\,f}(0°,\cos^2(\theta_{p\text{-}13f}/2)\cdot\cos^2(\theta_{p\text{-}10}/2)$

exiting transitional segment 15u.

DARK WAVE: In the segment 15u condensation process the electron wave loses a probability

$\Delta P=\cos^2(\theta_{p\text{-}10}/2)-\cos^2(\theta_{p\text{-}13f}/2)\cdot\cos^2(\theta_{p\text{-}10}/2)$

$\quad = \sin^2(\theta_{p\text{-}13f}/2)\cdot\cos^2(\theta_{p\text{-}10}/2)$.

That ΔP is manifested as the probability $P_{D2\text{-}15u\,f}$ of a second dark (empty) wave entity "D2" that is generated in the same manner as D1 in transitional segment 11. Accordingly,

$\Psi_{D2\text{-}15u\,f}(\theta_{D2\text{-}\delta\text{-}15u\,f},P_{D2\text{-}15u\,f})=\Psi_{D2\text{-}15u\,f}(180°,\sin^2(\theta_{p\text{-}13f}/2)\cdot\cos^2(\theta_{p\text{-}10}/2))$.

represents the D2 exiting segment 15u as a free empty δ-form spinor.

QuWT

OCCUPIED WAVE: There are minor differences to be noted with respect to the segment 15u process compared to that of 11. The $\partial_y B$ gradient encountered in segment 15u is negative rather than positive. However, as noted earlier the Q_e criterion is based upon the temporal magnitude of magnetic field change and not the sign of that change. Additionally, since $\boldsymbol{\mu}_e$ is already anti-aligned with **B** as the uniform amplitude spin structure wave entered segment 15u, the orientation of $\boldsymbol{\mu}_e$ is unchanged as condensation to δ-form concludes within segment 15u. Effectively, the directional quantization that was induced in segment 11 is still present throughout segment 15u. Because the longitudinal gradient $\partial_y B$ is negative in the distal region of segment 15u, the electron Ag atom system is accelerated relative to D2 and the two entities progressively separate.

DARK WAVE: The free empty Gaussian wave packet D1 on segment 14 enters transitional segment 15 as

$$\Psi_{D1\text{-}15i} = \Psi_{D1\text{-}14}$$

$$= \Psi_{D1\text{-}15i}(\theta_{D1\text{-}p\text{-}13f}, \sin^2(\theta_{p\text{-}10}/2))$$

and condensation within transitional segment 15 as Q_e is exceeded generates two contiguous δ-forms

$$\Psi_{D1d\text{-}15f}(180°, \sin^2(\theta_{D1\text{-}p\text{-}13f}) \cdot \sin^2(\theta_{p\text{-}10}/2))$$

and

$$\Psi_{D1u\text{-}15f}(0°, \cos^2(\theta_{D1\text{-}p\text{-}13f}) \cdot \sin^2(\theta_{p\text{-}10}/2))$$

respectively representing the dark pair D1d and D1u. Importantly, the pair remains contiguous as it propagates in the distal region of segment 15 with constant velocity, dynamically unaltered by the increasing magnitude of the longitudinal gradient $\partial_y B$.

OCCUPIED WAVE: By analogies to the analyses to this point we can immediately construct the electron Ag atom system wave functions for the remaining segments 16, 17, and 18 modified only by minor subsidiary considerations. Similarly, the wave functions for the dark D1d, D1u, and D2 entities can also be immediately constructed.

QuWT

The sequence of electron wave functions for the electron Ag atom system are the occupied δ-forms on the 5s orbital

$\Psi_{e\text{-}16u}=\Psi_{e\text{-}15u\,f}$

$\quad\quad =\Psi_{e\text{-}16u}(0°,\cos^2(\theta_{p\text{-}13f}/2)\cdot\cos^2(\theta_{p\text{-}10}/2)$

and

$\Psi_{e\text{-}17u\,i}=\Psi_{e\text{-}16u}$

$\quad\quad\quad =\Psi_{e\text{-}17u\,i}(0°,\cos^2(\theta_{p\text{-}13f}/2)\cdot\cos^2(\theta_{p\text{-}10}/2)$

Transitioning in segment 17 to a uniform occupied wave on the 5s orbital wave

$\Psi_{e\text{-}17u\,f}(\theta_{p\text{-}17u\,f},\theta_{M\text{-}17u\,f},\cos^2(\theta_{p\text{-}13f}/2)\cdot\cos^2(\theta_{p\text{-}10}/2))$

that continues in the same state on segment 18 as

$\Psi_{e\text{-}18u}(\theta_{p\text{-}17u\,f},\theta_{M\text{-}17u\,f},\cos^2(\theta_{p\text{-}13f}/2)\cdot\cos^2(\theta_{p\text{-}10}/2))$.

Segment 17 is associated with an emission process generating a polar orientation $\theta_{p\text{-}17u\,f}$ analogous to the segment 13 emission process. However, in the segment 17 process the evolution from a δ-form spinor to spinors forming spin structures occurs in a negligible B field unlike the segment 13 emission process B field. As a consequence, the electron, initially located on the 0° oriented δ-form spinor, is disrupted by the spinor evolution process and randomly moves to a constituent spinor at $\theta_{M\text{-}17u\,f}$ (where $\boldsymbol{\mu}_e$ has a polar orientation $\theta_{M\text{-}17u\,f}+180°$) since the associated energy of $\boldsymbol{\mu}_e\bullet\mathbf{B}{\sim}0$ for negligible B.

Over the total course of transit the electron Ag atom system is continuously directionally quantized from the distal region of segment 11 to the proximal region of segment 17. As a consequence of the longitudinal gradient $\partial_y B$, the system's energy loss over the distal region of segment 11 to the proximal region of segment 13 is equal and opposite its energy gain over the distal region of segment 15 to the proximal region of segment 17. As a result, the system's final velocity component along the y axis on segment 18u is substantially identical to its initial segment 10 velocity.

DARK WAVE: Those energies are relevant to the system's relative separation from extracted dark waves as depicted in Fig. 9. There is an

inclusive region extending from the distal region of segment 13 to the proximal region of segment 15 that is free of a significant longitudinal gradient. Over that inclusive region the decelerated system is increasingly retarded along the y axis relative to the dark D1, and a net retardation along the y axis is still present as the system and D1 reach segments 18u and 18 respectively despite the system's energy restoration. Concurrently, the system's energy gain increasingly separates it from the dark entity D2 extracted from the system in segment 17u as the two entities continue along segment 18u.

The states of the D1d and D1u contiguous, anti-aligned dark δ-form spinors emerging from the distal region of segment 15 are the same as their respective states on segment 16

$\Psi_{D1d-16}(180°, \sin^2(\theta_{D1-p-13f}) \cdot \sin^2(\theta_{p-10}/2))$

and

$\Psi_{D1u-16}(0°, \cos^2(\theta_{D1-p-13f}) \cdot \sin^2(\theta_{p-10}/2))$

and similarly as they enter transitional segment 17

$\Psi_{D1d-17i} = \Psi_{D1d-16}$

and

$\Psi_{D1u-17i} = \Psi_{D1u-16}$.

D1d and D1u continue to propagate contiguously in segment 16 and in the proximal region of transitional segment 17 since they are both unaffected by $\partial_y B$.

As D1d and D1u transit through $<Q_e$ within segment 17 the two δ-forms resolve back toward a single evolving dark wave packet in the distal region of segment 17 with a final resultant on that segment

$\Psi_{D1-17f}(\theta_{D1-p-13f}, \sin^2(\theta_{p-10}/2))$

and on segment 18 an equivalent

$\Psi_{D1-18}(\theta_{D1-p-13f}, \sin^2(\theta_{p-10}/2))$.

QuWT

These resultant forms are identical to $\Psi_{D1\text{-}13f}$ from which D1d and D1u were derived. Accordingly, the resultant state of the two resolved δ-forms is appropriately identified as the dark D1.

This entire process of the δ-form resolution has strong LR analogs in the present analyses of particle states and also in the LR analysis of photon states.

The resolution of orthogonal δ-forms into a fully formed wave

$$\Psi_{D1d\text{-}16}(180°, \sin^2(\theta_{D1\text{-}p\text{-}13f}) \cdot \sin^2(\theta_{p\text{-}10}/2)) + \Psi_{D1u\text{-}16}(0°, \cos^2(\theta_{D1\text{-}p\text{-}13f}) \cdot \sin^2(\theta_{p\text{-}10}/2)) \rightarrow \Psi_{D1\text{-}17f}(\theta_{D1\text{-}p\text{-}13f}, \sin^2(\theta_{p\text{-}10}/2))$$

occurs as the two contiguous δ-forms pass from a region with $>Q_e$ to a region with $<Q_e$. This transition is the direct analog of the time-reversed process

$$\Psi_{e\text{-}11f}(0°, \cos^2(\theta_{p\text{-}10}/2)) + \Psi_{D1\text{-}11f}(180°, \sin^2(\theta_{p\text{-}10}/2)) \rightarrow \Psi_{e\text{-}11i}(\theta_{p\text{-}10}, \theta_{M\text{-}10}, 1)$$

in which two contiguous, orthogonal δ-forms pass from a region with $>Q_e$ to a region with $<Q_e$ and resolve to a fully formed wave.

The present resolution of orthogonal δ-forms also has a direct LR analog with photon traversal of a loop such as opposed calcite crystals. In that traversal we have shown that a loop-incident photon is split onto two separate paths baring respectively an occupied δ-form wave and an orthogonal, empty (dark) δ-form wave. At the exit face of the loop the resultant of the two waves combining is a fully formed photon wave packet with an arc bisector orientation θ_a and a probability identical to that of the incident photon. If the incident photon is replaced by an incident empty wave packet, the resultant wave packet exiting the loop is identical to that incident empty wave packet.

The progression of D2 beyond segment 15u is straightforward. Because

$$\Psi_{D2\text{-}16u} = \Psi_{D2\text{-}17u\,i} = \Psi_{D2\text{-}15u\,f},$$

the wave functions for segments 16u and 17u i are respectively

$$\Psi_{D2\text{-}16u}(180°, \sin^2(\theta_{p\text{-}13f}/2) \cdot \cos^2(\theta_{p\text{-}10}/2))$$

and

$$\Psi_{D2\text{-}17u\,i}(180°, \sin^2(\theta_{p\text{-}13f}/2) \cdot \cos^2(\theta_{p\text{-}10}/2)).$$

Transit within segment 17 results in evolution to a full wave packet as an emission process yielding

$\Psi_{D2\text{-}17uf}(\theta_{D2\text{-}p\text{-}17uf}, \sin^2(\theta_{p\text{-}13f}/2)\cdot\cos^2(\theta_{p\text{-}10}/2))$

and, on segment 18, an identical

$\Psi_{D2\text{-}18u}(\theta_{D2\text{-}p\text{-}17uf}, \sin^2(\theta_{p\text{-}13f}/2)\cdot\cos^2(\theta_{p\text{-}10}/2))$

where $\theta_{D2\text{-}p\text{-}17uf}$ is the orientation of a random member of a 180° polarization ensemble.

3.8 CONCLUSIONS

The above analysis of LR wave states in the SGE shows that its most notable characteristic, that of directional quantization, occurs before the electron Ag atom system enters the SGE magnet perimeter.

For LR, the condensation process of electron wave packets entering the longitudinal gradient field of the SGE magnet is analogous to the condensation process of photon wave packets entering a two-channel calcite polarizer. However, from the perspective of classical physics, the sorting of photons onto one or the other of the calcite output channels presents no self-evident conundrum unlike the sorting of electrons (and their coupled atoms) onto one or the other of two discrete SGE magnet output channels. For the SGE, that conundrum arises because of the apparent absence of an applied force and an energy exchange mechanism with regard to the electron's magnetic moment.

A possible solution to this conundrum was considered in a paper by Einstein and Ehrenfest [382-383] shortly after SGE. They postulated that transitions occurred to up or down quantum states as the atoms transited the high vertical gradient region within the perimeter of the magnet poles but concluded that the quantum transition times were far too slow to account for the observed results of SGE.

That unresolved conundrum was avoided in PI by assigning a probabilistic nature to entities such as an electron whereby a measurement process conducted along a particular magnetic field axis ad hoc provides a quantized up or down state alignment. In this regard the SGE results are widely

recognized as constituting a phenomenon that distinctly departs from classical physics.

In contrast, in the LR representation of SGE the electron's final magnetic moment alignment in a particular SGE apparatus is fully deterministic from the instant the atom leaves the SGE beam source. In LR the electron is an objectively real entity that has some definite polar θ_p orientation of its spin structures as it leaves the source. Identifying only that θ_p is >90° or <90° then fully determines the final magnetic moment alignment. As the atom and its appended electron approach the SGE apparatus, a high longitudinal magnetic gradient exterior to the SGE magnet is suddenly encountered. It is that sudden encounter that begins the process of projective condensation

The process of magnetic moments rotating to alignment with the magnetic field is independent of the transverse high gradient magnetic field within the perimeter of the SGE magnet poles. In LR the rotation is treated semi-classically arising from "quantum" forces that occur during projective condensation of the wave structure upon suddenly encountering a significant longitudinal gradient outside the magnet pole perimeter where the transverse gradient field is negligible but the longitudinal gradient field is consequential.

The resultant spin up and spin down "states" of the magnetic moments are then recognized as distinct from formal quantum states such as those associated with atomic orbitals.